Cancer Cell
Article

Direct Signaling between Platelets and Cancer Cells Induces an Epithelial-Mesenchymal-Like Transition and Promotes Metastasis

Myriam Labelle,[1] Shahinoor Begum,[1] and Richard O. Hynes[1,*]
[1]Howard Hughes Medical Institute, Koch Institute for Integrative Cancer Research, Massachusetts Institute of Technology, Cambridge, MA 02139, USA
*Correspondence: rohynes@mit.edu
DOI 10.1016/j.ccr.2011.09.009

SUMMARY

Interactions of cancer cells with the primary tumor microenvironment are important determinants of cancer progression toward metastasis but it is unknown whether additional prometastatic signals are provided during the intravascular transit to the site of metastasis. Here, we show that platelet-tumor cell interactions are sufficient to prime tumor cells for subsequent metastasis. Platelet-derived TGFβ and direct platelet-tumor cell contacts synergistically activate the TGFβ/Smad and NF-κB pathways in cancer cells, resulting in their transition to an invasive mesenchymal-like phenotype and enhanced metastasis in vivo. Inhibition of NF-κB signaling in cancer cells or ablation of TGFβ1 expression solely in platelets protects against lung metastasis in vivo. Thus, cancer cells rely on platelet-derived signals outside of the primary tumor for efficient metastasis.

INTRODUCTION

The dynamic crosstalk between tumors and their microenvironment is increasingly recognized as a key regulator of malignant progression. Tumor cells are known to secrete several cytokines, which activate stromal fibroblasts and induce the recruitment of immune cells to the tumor. In turn, signals provided by the local microenvironment promote the ability of tumor cells to invade and metastasize (Joyce and Pollard, 2009). In primary carcinomas, secreted growth factors and cytokines contributed by stromal cells are key in inducing epithelial-mesenchymal transition (EMT), a transient and reversible process that promotes cell motility, invasion, and dissemination of cancer cells out of the tumor microenvironment (Scheel et al., 2007; Thiery, 2002). Subsequently, tumor cells travel through the bloodstream before arresting and extravasating in a new microenvironment (secondary site). Some current models of tumor progression propose that the metastatic potential of tumor cells is entirely shaped at the primary tumor site, with few or no signaling events occurring during the intravascular transit of tumor cells. Considering that multiple growth factors and cytokines are released in the bloodstream, cancer cells may sense additional signaling cues outside of the primary microenvironment. However, it is unclear whether circulating cancer cells require additional instructive signals for effective metastasis, either while in the circulation or on arrival at the secondary site.

Among the multitude of different signaling molecules found in the blood, transforming growth factor-beta (TGFβ) is known to promote metastasis by enhancing EMT and invasiveness in primary carcinomas (Oft et al., 1998). Furthermore, inhibition of the ability of tumor cells to respond to TGFβ (by overexpression of dominant-negative TGFβ receptor II) reduces intravasation and metastatic seeding in the lungs (Biswas et al., 2007; Padua et al., 2008; Siegel et al., 2003) as well as the development of bone metastases (Yin et al., 1999). In particular, upon dissemination to the bones, tumor cells activate osteoclasts to degrade the bone matrix and release the stored TGFβ, which in turn leads to enhanced tumor cell malignancy (Kang et al., 2005). However,

Significance

The host-to-tumor signaling events governing cancer metastasis are poorly understood. We explored the possibility that the metastatic potential of tumor cells is modulated during their transit through the bloodstream. Our findings indicate that direct contact with platelets primes tumor cells for metastasis, and induces an epithelial-mesenchymal-like transition via synergistic activation of both the TGFβ and NF-κB pathways. Specific ablation of platelet-derived TGFβ or NF-κB signaling in cancer cells prevents metastasis. Globally, our study reveals that the metastatic potential of tumor cells continues to evolve outside the primary tumor site, in response to tumor-host interactions in the bloodstream. Platelet-tumor cell interactions and the signaling pathways that they trigger are therefore crucial determinants of cancer metastasis and potential targets for anti-metastatic therapies.

in the case of metastasis to other tissues such as the lungs, the source of TGFβ bioavailable to tumor cells at the site of metastatic seeding remains unknown.

Platelets contain a plethora of growth factors and cytokines, including high concentrations of TGFβ (Assoian et al., 1983). Thus, platelet-derived factors could potentially be involved in the promotion of a metastatic phenotype. Consistent with a role of platelets in metastasis, defective platelet function or reduced platelet counts have been associated with decreased metastasis formation in various transgenic mouse models (Bakewell et al., 2003; Camerer et al., 2004; Gasic et al., 1968; Kim et al., 1998). The prometastatic effects of platelets have so far been attributed to their ability to promote adhesion or to their capacity to prevent cell death in the circulation by forming a physical shield around tumor cells. This shield protects tumor cells from natural killer cell-mediated lysis (Nieswandt et al., 1999; Palumbo et al., 2005), limits their exposure to shear stress, and promotes their adhesion to the endothelium (Erpenbeck and Schön, 2010; Gay and Felding-Habermann, 2011; Im et al., 2004; Jain et al., 2007; Karpatkin et al., 1988; Sierko and Wojtukiewicz, 2007). In addition, it is possible that platelets provide instructive signals that affect tumor cell behavior and metastatic potential.

In this study, we have tested whether platelets can provide a signaling platform for cancer cells outside of the primary tumor in the context of metastasis.

RESULTS

Platelets Prime Tumor Cells For Metastasis

To investigate whether platelets can have a direct impact on tumor cell behavior, we tested whether platelets could prime tumor cells for metastasis. Colon carcinoma cells (MC38GFP; isolated from a grade III carcinoma chemically induced in a C57BL/6 mouse) (Corbett et al., 1975) or breast carcinoma cells (Ep5 [EpRas]; spontaneously immortalized mouse mammary epithelial cell line transformed by the v-Ha-Ras oncogene) (Oft et al., 1996) were coincubated with purified platelets for 40 hr in vitro. Platelets were then washed away, and tumor cells (substantially devoid of any platelets; see Figure S1A available online) were injected into the tail veins of mice. Pretreating either MC38GFP or Ep5 cells with platelets led to a marked increase in the number of metastatic foci in the lungs 14 days after tail-vein injection (Figure 1A). The increase in metastasis was presumably due to the enhanced capacity of MC38GFP and Ep5 cells to seed the lungs as demonstrated by increased numbers of cells present after 48 hr (Figure 1B). These results indicate that a transient interaction between tumor cells and platelets in vitro is sufficient to increase tumor cell metastatic seeding.

Treatment of Tumor Cells with Platelets Induces an Invasive Mesenchymal-Like Phenotype

We next sought to define the molecular mechanisms induced by platelet-tumor cell interactions that could mediate the increased metastatic capacity of tumor cells. In tissue culture, both MC38GFP and Ep5 tumor cell lines underwent morphological changes reminiscent of an epithelial-mesenchymal transition (EMT) when treated with platelets for 24 hr (Figure 1C). Analysis of mesenchymal markers and transcription factors involved in EMT revealed that the mRNA expression of *snail* (*Snai1*), *vimentin* (*Vim*), *fibronectin* (*Fn1*), and *plasminogen activator inhibitor-1* (*PAI-1*; *Serpine1*) was consistently upregulated, whereas the epithelial marker *claudin 1* (*Cldn1*) was downregulated in platelet-treated cells (Figure 1D). E-cadherin protein levels were also reduced in platelet-treated Ep5 cells in comparison with controls (Figure 1E; Figure S1B), whereas N-cadherin was relocalized from cell-cell junctions to the cytoplasm (Figure S1B). In addition, zymography revealed increased matrix metalloproteinase-9 (MMP-9) secretion following exposure to platelets (Figure 1F), suggesting a higher capacity to degrade the extracellular matrix (ECM) and to invade the surrounding environment. In agreement with these findings, the human breast epithelial cell lines MCF10A and HMLER also displayed a more mesenchymal morphology upon exposure to platelets (Figure S1C), together with increased expression of EMT-associated genes and MMP-9 secretion (Figures S1D and S1E). Thus, platelets induce EMT-like features also in epithelial cells of human origin.

To test directly whether EMT-like morphological and molecular changes promote an invasive behavior, we seeded platelet-treated MC38GFP and Ep5 cells on Matrigel-coated transwells and detected increased invasion in comparison with untreated cells (Figure 1G). Altogether these results show that platelets promote the adoption of a more mesenchymal and invasive phenotype by tumor cells.

Platelets Promote Activation of the TGFβ/Smad Pathway in Tumor Cells

To gain better insight into the signaling pathways involved in platelet-to-tumor cell communication, we defined the platelet-induced gene expression signature by microarray analysis. For this purpose, gene expression profiles of Ep5 cells treated for 24 hr with platelets or buffer alone (untreated) were compared. Any contribution of platelet mRNA was excluded from the platelet-induced gene signature by performing a microarray with platelets alone (see Experimental Procedures and Figure 2A). Only 21 mRNAs were contributed at significant levels by the platelets and were excluded from subsequent analyses. Among the most highly upregulated genes in tumor cells, we found several genes known to play prominent roles in EMT, ECM remodeling, and the promotion of metastasis (e.g., *Mmp9*, *Serpine1* (*PAI-1*), *Fn1*, *Jag1*, *Vegfc*, *Vim*, *Edn1*, *Vegfa*, *Ctgf*) (Tables S1 and S2). Bioinformatic analysis using GeneGo canonical pathway maps (Figure 2B) and gene set enrichment analysis (GSEA) (Table 1) confirmed that platelets strongly activate EMT-related genes and revealed TGFβ-dependent pathways as being the most significantly upregulated following platelet treatment (Figure 2B). Interestingly, GSEA analyses further revealed that previously defined gene signatures associated with cancer stem cells, poor prognosis and metastasis are also enriched in platelet-treated cells, suggesting that platelets induce an overall more aggressive phenotype in tumor cells (Table 1).

Considering that a prolonged exposure to TGFβ promotes EMT in many cancer cell lines, including Ep5 cells (Derynck and Akhurst, 2007; Maschler et al., 2005; Oft et al., 1996), we investigated whether platelet-derived TGFβ could activate TGFβ/Smad signaling in tumor cells. We found increased levels of active and latent TGFβ1 in the medium derived from the coculture of tumor cells and platelets, after the platelets were removed (Figure 2C). Ep5 and MC38GFP cells treated with

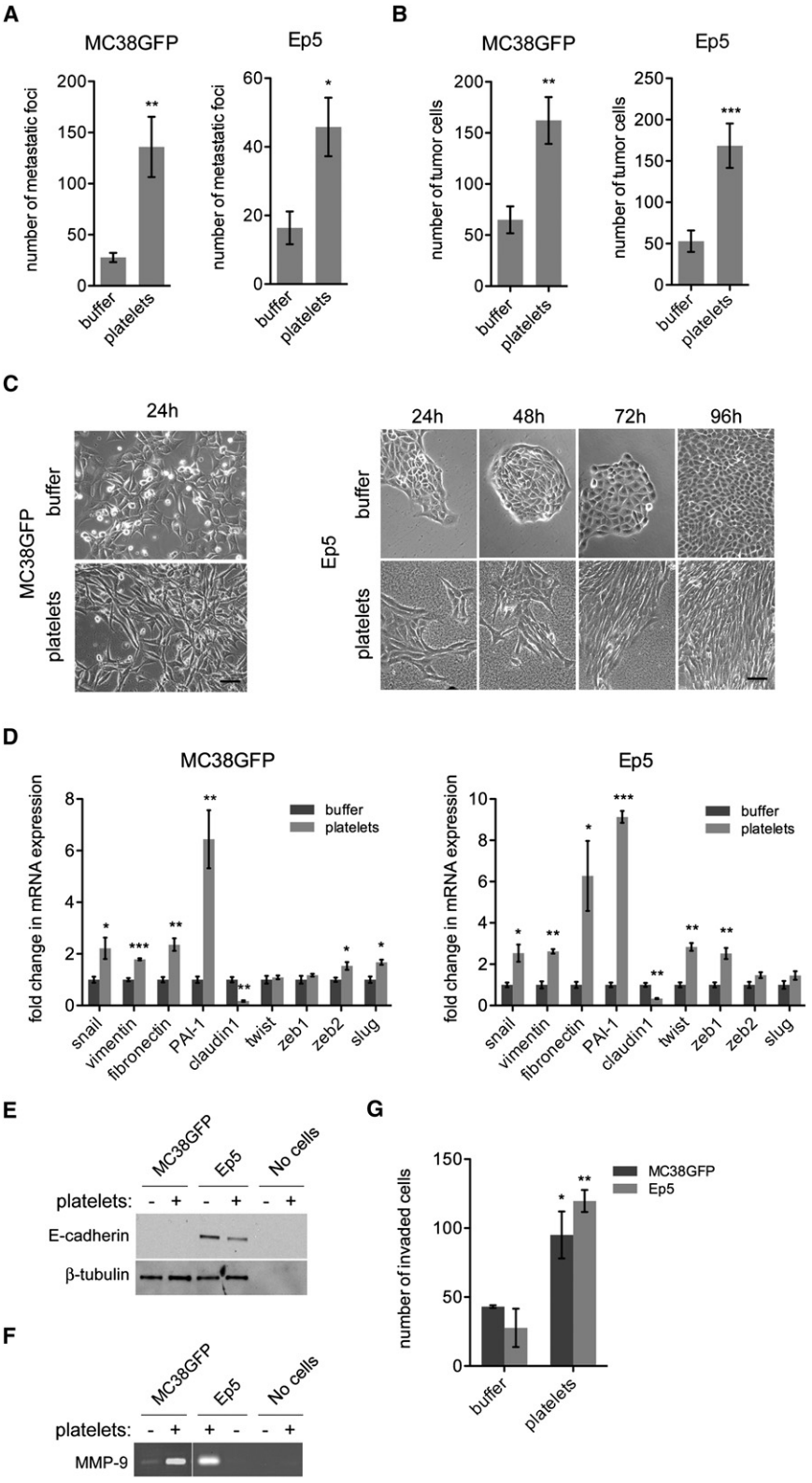

Figure 1. Pretreatment of Tumor Cells with Platelets Promotes Lung Metastasis by Increasing Tumor Cell Seeding and Inducing an EMT-Like Invasive Phenotype

(A) Numbers of metastatic foci at the surface of lungs (two largest lobes) 14 days after tail-vein injection of MC38GFP cells or Ep5 cells stably expressing ZsGreen (Ep5-ZsGreen) pretreated with buffer (vehicle) or platelets for 40 hr (n = 5–12).

(B) Numbers of tumor cells at the surface of lungs 48 hr after tail-vein injection of MC38GFP or Ep5-ZsGreen cells pretreated with buffer or platelets for 40 hr (n = 6–11).

(C) Phase-contrast micrographs of MC38GFP or Ep5 cells treated with buffer or platelets for the times indicated. Scale bar represents 50 μm.

(D) Relative fold change in mRNA expression in MC38GFP or Ep5 cells treated with buffer or platelets for 40 hr (n = 3). Values are normalized to *Gapdh* expression.

(E) Detection of E-cadherin protein levels by immunoblotting of lysates of MC38GFP or Ep5 cells treated as in (D). Amounts of platelets equal to those used to treat cells were also loaded as control (no cells). β-tubulin was used as loading control.

(F) Zymography for MMP-9 in the conditioned medium of MC38GFP or Ep5 cells treated as in (D). Amounts of platelets equal to those used to treat cells were also loaded as control (no cells).

(G) MC38GFP and Ep5 cells were added at the top of transwells coated with Matrigel and treated with buffer or platelets. The total number of cells that invaded to the bottom of the transwell was counted after 48 hr (n = 3).

For (A), (B), (D), and (G) bars represent the mean ± SEM. *p < 0.05, **p < 0.01, ***p < 0.001 were determined by Student's t test. See also Figure S1.

platelets also showed increased phosphorylation of the TGFβ signaling effector Smad2 (Figure 2D) and Smad-binding element (SBE)-dependent transcription (Figure 2E) compared with controls, demonstrating that interaction with platelets induces TGFβ/Smad signaling in tumor cells. We next investigated whether platelet-induced tumor cell invasion is dependent on TGFβ signaling. Interestingly, adding a TGFβRI inhibitor (SB431542) or a TGFβ1 blocking antibody abolished platelet-induced cell invasion (Figure 2F). Treatment with SB431542 also inhibited the upregulation of EMT markers induced by platelets in Ep5 and MC38GFP cells (Figure 2G). Thus, platelet-derived TGFβ induces a prometastatic invasive phenotype in tumor cells via activation of the TGFβ/Smad signaling pathway.

Platelet-Derived TGFβ1 Is Necessary for Metastasis In Vivo

To test directly the specific contribution of platelet-derived TGFβ1 to metastasis in vivo, *Pf4-cre* mice (Tiedt et al., 2007) were crossed with *TGFβ1*$^{fl/fl}$ mice (Li et al., 2007) to generate mice lacking TGFβ1 specifically in their megakaryocytes and platelets. *Pf4-cre*$^{+}$;

TGFβ1$^{fl/fl}$ mice had normal bleeding times and platelet counts (Table S3), showing that platelet hemostatic functions are not impaired in these mice. ELISA for TGFβ1 showed that platelets from *Pf4-cre*$^{+}$; *TGFβ1*$^{fl/fl}$ mice contained <1% of the amount of TGFβ1 present in platelets from wild-type (WT) mice (Figure 3A), confirming that *Pf4-cre*$^{+}$; *TGFβ1*$^{fl/fl}$ mice could be used to study the role of platelet-derived TGFβ1 in metastasis. Furthermore, the concentration of TGFβ1 was significantly lower in platelet-rich plasma from *Pf4-cre*$^{+}$; *TGFβ1*$^{fl/fl}$ mice compared with plasma from WT mice (Figure 3A), suggesting that platelets are a major source of TGFβ1 in the circulation.

We next tested whether platelets lacking TGFβ1 could induce Smad signaling in vitro and found a decrease in SBE-dependent luciferase reporter activity (Figure 3B) and MMP-9 secretion by Ep5 cells, in comparison with treatment with WT platelets (Figure 3C). Thus, although other members of the TGFβ family might be secreted by platelets, these results suggest that platelet-derived TGFβ1 is key for the platelet-induced activation of Smad signaling in cancer cells.

To test the role of platelet-derived TGFβ1 during metastasis in vivo, MC38GFP cells were injected into *Pf4-cre*$^{+}$; *TGFβ1*$^{fl/fl}$ or WT mice via the tail vein. Fourteen days after injection, the numbers of metastases present in the lungs of *Pf4-cre*$^{+}$; *TGFβ1*$^{fl/fl}$ mice were greatly reduced compared with those in littermate controls (WT and *Pf4-cre*$^{+}$; *TGFβ1*$^{fl/+}$ mice) (Figures 3D and 3E). Importantly, cells pretreated with platelets from WT mice and injected into *Pf4-cre*$^{+}$; *TGFβ1*$^{fl/fl}$ mice also formed significantly fewer metastases than platelet-treated cells injected into WT mice (Figure 3F). Conversely, pretreating tumor cells with TGFβ1-deficient platelets led to the formation of significantly fewer metastases in WT mice, in comparison to cells pretreated with platelets from WT mice (Figure 3F; see Figure S1A for micrographs of injected cells). Thus, whereas a platelet pretreatment primes tumor cells for metastasis in WT mice in a TGFβ1-dependent manner, the presence of platelet-derived TGFβ1 in the host bloodstream is also required for efficient metastasis.

We next investigated the role of platelet-derived TGFβ1 in the early steps in the seeding of metastases. Whereas equivalent numbers of cells were found in the lungs 3 hr after injection for both WT and *Pf4-cre*$^{+}$; *TGFβ1*$^{fl/fl}$ mice (Figure 3G), significantly lower numbers of cells remained in the lungs after 21 hr or 48 hr in *Pf4-cre*$^{+}$; *TGFβ1*$^{fl/fl}$ mice (Figure 3G). Closer inspection by confocal microscopy and 3D-rendering of lungs revealed that, at 3 hr postinjection, tumor cells were mainly present within the blood vessels (Figures 3H and 3I) in association with platelets (Figure 3J), whereas after 48 hr they were found mainly outside of the blood vessels in both WT and *Pf4-cre*$^{+}$; *TGFβ1*$^{fl/fl}$ mice (Figures 3H and 3I). Interestingly, at the intermediate time point of 21 hr, tumor cells were found both in the intravascular and extravascular compartments, and a smaller proportion of cells were localized extravascularly in the lungs of *Pf4-cre*$^{+}$; *TGFβ1*$^{fl/fl}$ mice compared with WT, suggesting that tumor cell extravasation is impaired in *Pf4-cre*$^{+}$; *TGFβ1*$^{fl/fl}$ mice (Figure 3H).

Because another gene (*stumpy*) was also targeted in the *TGFβ1*$^{fl/fl}$ mice (Li et al., 2007; Town et al., 2008), we generated *Pf4-cre*$^{+}$; *TGFβ1*$^{fl/-}$ and *TGFβ1*$^{fl/-}$ mice, with one null allele of *TGFβ1*, which allows expression of one WT allele of *stumpy* in these mice. The numbers of metastases observed in lungs of *TGFβ1*$^{fl/-}$ mice after 14 days were similar to those obtained for WT or *Pf4-cre*$^{+}$; *TGFβ1*$^{fl/+}$ mice, whereas *Pf4-cre*$^{+}$; *TGFβ1*$^{fl/-}$ mice had reduced numbers of metastases (Figure S2). These results show that the reduction in metastasis is not due to the deletion of *stumpy*, but attributable to the lack of TGFβ1. Altogether, our data reveal that platelet-derived TGFβ1 plays an important role in promoting metastatic seeding in the lungs possibly by inducing extravasation and invasion into the lung parenchyma.

Platelet-Derived TGFβ1 and Platelet-Bound Factors Cooperate to Promote Metastasis

Considering that TGFβ1 is a secreted factor released by platelets upon activation (Assoian and Sporn, 1986), we next asked whether exposure to the releasate from activated platelets would be sufficient to prime tumor cells for metastasis in vivo. Platelets were therefore activated with thrombin and the releasate was separated from the exhausted platelets by centrifugation (neither thrombin nor its inhibitor hirudin affected tumor cell behavior in our system) (Figures S3A–S3C). Higher concentrations of active TGFβ1 were measured in the conditioned medium of tumor cells treated with the releasate than with the pellet from activated platelets, whereas similar amounts of total TGFβ1 were found in the conditioned medium of tumor cells treated with either fraction (Figure 4A). Furthermore, similar levels of Smad2 phosphorylation (Figure 4B) and SBE-based TGFβ reporter activity were induced in tumor cells incubated with the releasate or the pellet (Figure 4C), demonstrating that the concentration of TGFβ1 present in either fraction is sufficient to induce Smad signaling to comparable levels.

However, despite the higher concentrations of TGFβ1 present in the conditioned medium of tumor cells treated with the platelet releasate (Figure 4A), increased numbers of lung metastases were observed only when tumor cells were preincubated with the pellet fraction but not with the releasate from activated platelets (Figure 4D). Additionally, tumor cell retention in the lungs was increased 48 hr after tail-vein injection when cells were pretreated with platelets or the pellet fraction but not after treatment with the releasate (Figure 4E). Consistent with these results, cells adopted a more mesenchymal morphology (Figure 4F) and showed higher expression of prometastatic genes (Figure 4G; Figure S3D), increased secretion of MMP-9 (Figure 4H), and increased invasion (Figure S3E) upon incubation with the platelet pellet fraction but not with the platelet releasate. Furthermore, microarray analysis of pellet- or releasate-treated Ep5 cells revealed that treatment with the pellet fraction induced gene expression changes very similar to those observed upon platelet treatment (Figures S3F and S3G). However, treatment with the platelet releasate resulted in only partial gene expression changes in comparison with treatment with either platelets or the pellet fraction (Figures S3F–S3I). Gene expression signatures associated with EMT and tumor progression were also robustly enriched in the pellet-treated cells but not in the releasate-treated cells (Table S4). Thus, platelet-induced effects on EMT, invasion, and metastasis are not mediated by secreted TGFβ alone, but also require additional platelet-bound factors. These data also suggest that these platelet-bound factors synergize with TGFβ to enhance metastasis.

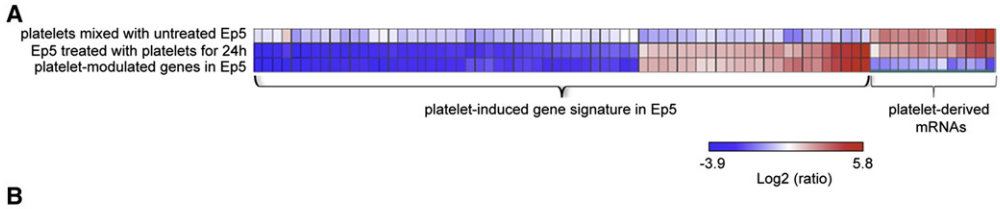

B

GeneGo canonical pathway	pValue
Development_Regulation of epithelial-to-mesenchymal transition (EMT)	5.79E-06
Development_TGF-beta-dependent induction of EMT via SMADs	1.40E-05
Development_TGF-beta-dependent induction of EMT via MAPK	7.94E-05
Cell adhesion_ECM remodeling	1.41E-04
Immune response_IL-17 signaling pathways	3.14E-04
Development_EGFR signaling pathway	4.10E-04
Transcription_Role of Akt in hypoxia induced HIF1 activation	7.38E-04
Development_IGF-1 receptor signaling	1.11E-03
ENaC regulation in airways	1.21E-03
Immune response_TREM1 signaling pathway	1.69E-03

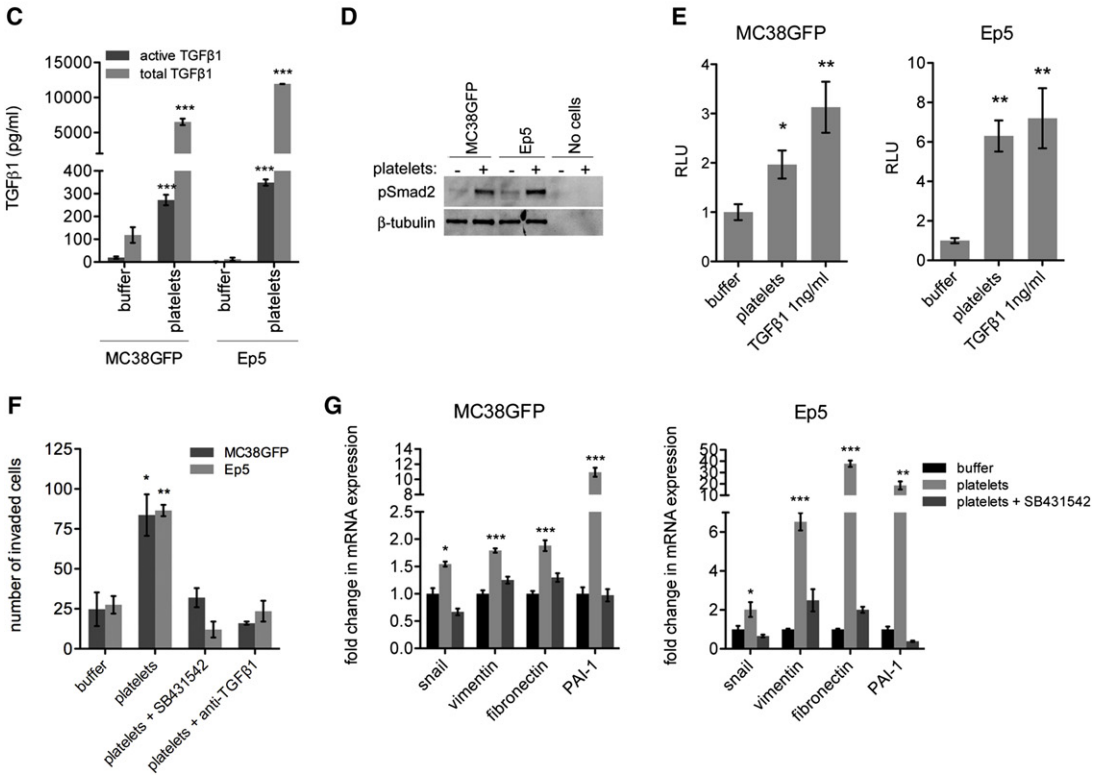

Figure 2. Platelet-Induced Gene Expression Signature Reveals Increased Expression of Prometastatic Genes and Activation of the TGFβ Pathway in Tumor Cells

(A) Heat map of genes regulated by >4-fold ($p < 0.05$) in Ep5 cells treated with platelets in comparison with untreated Ep5 cells (line 2). Line 1 and line 2 show Log2 ratios of gene expression compared to untreated Ep5 cells. mRNAs present in platelets (line 1) were removed from the list of genes modulated upon platelet treatment of Ep5 cells (line 2) to generate a platelet-induced gene signature (line 3), which is listed in Table S2.

(B) Canonical signaling pathways most significantly associated with the list of genes differentially expressed by Ep5 cells upon platelet treatment (platelet-induced gene signature; Table S1; threshold = 2-fold, up and downregulated genes considered, $p < 0.05$) as determined with GeneGo canonical pathway maps. The 10 pathways with the lowest p values are shown.

(C) Concentration of active and total TGFβ1 in conditioned medium from MC38GFP or Ep5 cells treated with buffer or platelets for 40 hr. The conditioned medium was collected, centrifuged to remove platelets, and the presence of TGFβ1 in the supernatant measured by ELISA. Each bar represents the mean ± SEM of n = 2–6. ***$p < 0.001$ as determined by Student's t test.

(D) Detection of phospho-Smad2 protein levels by immunoblotting of Ep5 or MC38GFP cells treated as in (C). Amounts of platelets equal to those used to treat cells were also loaded as control (no cells). β-tubulin is used as loading control.

(E) Relative luciferase activity (RLU) in MC38GFP or Ep5 cells stably expressing a luciferase reporter under the control of an SBE promoter and treated for 40 hr with buffer, platelets or 1ng/ml TGFβ1 (positive control) (n = 5–6). Each bar represents the mean ± SEM, and *$p < 0.05$, **$p < 0.01$ versus buffer were determined by one-way ANOVA followed by Tukey's posttest.

Table 1. Gene Set Enrichment Analysis for Ep5 Cells Treated with Platelets

Gene Sets	NES	Nominal p Value	FDR
EMT signatures			
BLICK_EMT-SIG_UP	1.993	<0.001	<0.001
TAUBE_EMT_UP	1.328	0.060	0.060
TAUBE_EMT_DN	−2.081	<0.001	<0.001
ONDER_CDH1_TARGETS_2_UP	1.526	<0.001	0.044
ONDER_CDH1_TARGETS_2_DN	−1.832	<0.001	0.006
TGFβ Signatures			
GIAMPIERI_TGFB_UP	1.992	<0.001	<0.001
GIAMPIERI_TGFB_DN	−2.576	<0.001	<0.001
VALCOURT_TGFB_UP	1.813	<0.001	0.005
VALCOURT_TGFB_DN	−1.926	<0.001	<0.001
Cancer stem cell signatures			
CREIGHTON_CSC_UP	1.675	<0.001	<0.001
CREIGHTON_CSC_DN	−1.778	<0.001	<0.001
Tumor progression and metastasis signatures			
VANTVEER_BREAST_CANCER_POOR_PROGNOSIS	1.953	<0.001	<0.001
JAEGER_METASTASIS_UP	1.875	<0.001	0.003

Enrichment of gene sets from the literature (see Supplemental Information for references). Positive NES indicates enrichment in platelet-treated Ep5 cells; negative NES indicates enrichment in untreated Ep5 cells. FDR, false discovery rate; NES normalized enrichment score.

TGFβ1 and Direct Platelet-Tumor Cell Contact Synergize to Promote Prometastatic Gene Expression

To test further whether platelets synergize with TGFβ signaling, we used the MLEC cell line stably expressing a luciferase reporter based on the promoter region of the TGFβ target gene *PAI-1* (Abe et al., 1994). These cells provide a specific readout for exogenous TGFβ bioavailability and signaling activity, and were therefore used to dissect the specific contribution of TGFβ signaling to the effects observed upon platelet treatment. Interestingly, we found that platelets induced higher luciferase activity than achievable with TGFβ1 treatment alone (Figure 5A). Furthermore, adding TGFβ1 together with platelets from either WT or *Pf4-cre*$^{+}$*; TGFβ1*$^{fl/fl}$ mice resulted in a synergistic activation of the *PAI-1* reporter that was completely blocked by adding either a TGFβRI inhibitor (SB431542) or an anti-TGFβ1 blocking antibody (Figure 5B). Moreover, separation of platelets (either resting or activated with thrombin) from the cancer cells by a semipermeable membrane blocked the synergistic activation of the *PAI-1* promoter (Figure 5C), inhibited the secretion of MMP-9 (Figure 5D), and abolished the upregulation of prometastatic genes in Ep5 and MC38GFP cells (Figure 5E). Taken together, these results show that platelet-derived TGFβ1 is necessary to induce the expression of several prometastatic genes and to promote metastasis in vivo but that, in addition, platelets provide other prometastatic signals that synergize with TGFβ signaling upon direct platelet-tumor cell contact.

The NF-κB Signaling Pathway Is Activated by Platelets in a Contact-Dependent Manner and Cooperates with TGFβ Signaling to Enhance Metastasis

We next sought to define the molecular pathway(s) induced upon platelet contact that cooperate with TGFβ to induce prometastatic gene expression and behavior. Using a set of luciferase reporter assays for several pathways involved in cancer, we screened for their activation in cancer cells in response to interaction with platelets. Interestingly, coincubation with platelets increased activation of the JNK and NF-κB pathways in Ep5 cells (Figure 6A). Whereas the JNK pathway seemed to be activated by the releasate, activation of the NF-κB pathway was increased only when cells were incubated with either platelets or the pellet fraction from activated platelets (Figure S4A). Ep5 cells stably expressing an NF-κB luciferase reporter also displayed increased luciferase activity upon treatment with platelets or activated platelet pellets but not if treated with the releasate (Figure 6B). Furthermore, secretion of MCP-1, a known target of the NF-κB pathway, was increased in the supernatant of Ep5 and MC38GFP tumor cells treated with platelets or the pellet fraction, further showing that platelet-bound factors activate the NF-κB pathway in tumor cells (Figure S4B). Notably, many of the genes found to be highly upregulated in the platelet-induced gene signature, such as *Ccl2* (*MCP-1*), *Mmp9*, *Vegfc*, *Tnc*, *Serpine1*, *Jag1*, and *Ncam1* have been previously reported as NF-κB target genes (Figure 2A; Table S1). Furthermore, GSEA analysis revealed that NF-κB-related

(F) MC38GFP and Ep5 cells were added at the top of transwells coated with Matrigel and treated with buffer, platelets, platelets + SB431542 (10 μM) or platelets + TGFβ1 blocking antibody (6 μg/ml). The total numbers of cells that invaded to the bottom of the transwell were counted after 48 hr (n = 3). Each bar represents the mean ± SEM, and *p < 0.05, **p < 0.01 versus buffer were determined by one-way ANOVA followed by Tukey's posttest.
(G) Relative fold change in mRNA expression in MC38GFP or Ep5 cells treated with buffer, or platelets +/− SB431542 (10 μM) for 40 hr (n = 3). Values are normalized to *Gapdh* expression. Each bar represents the mean ± SEM, and *p < 0.05, **p < 0.01, ***p < 0.001 versus buffer were determined by one-way ANOVA followed by Tukey's posttest.

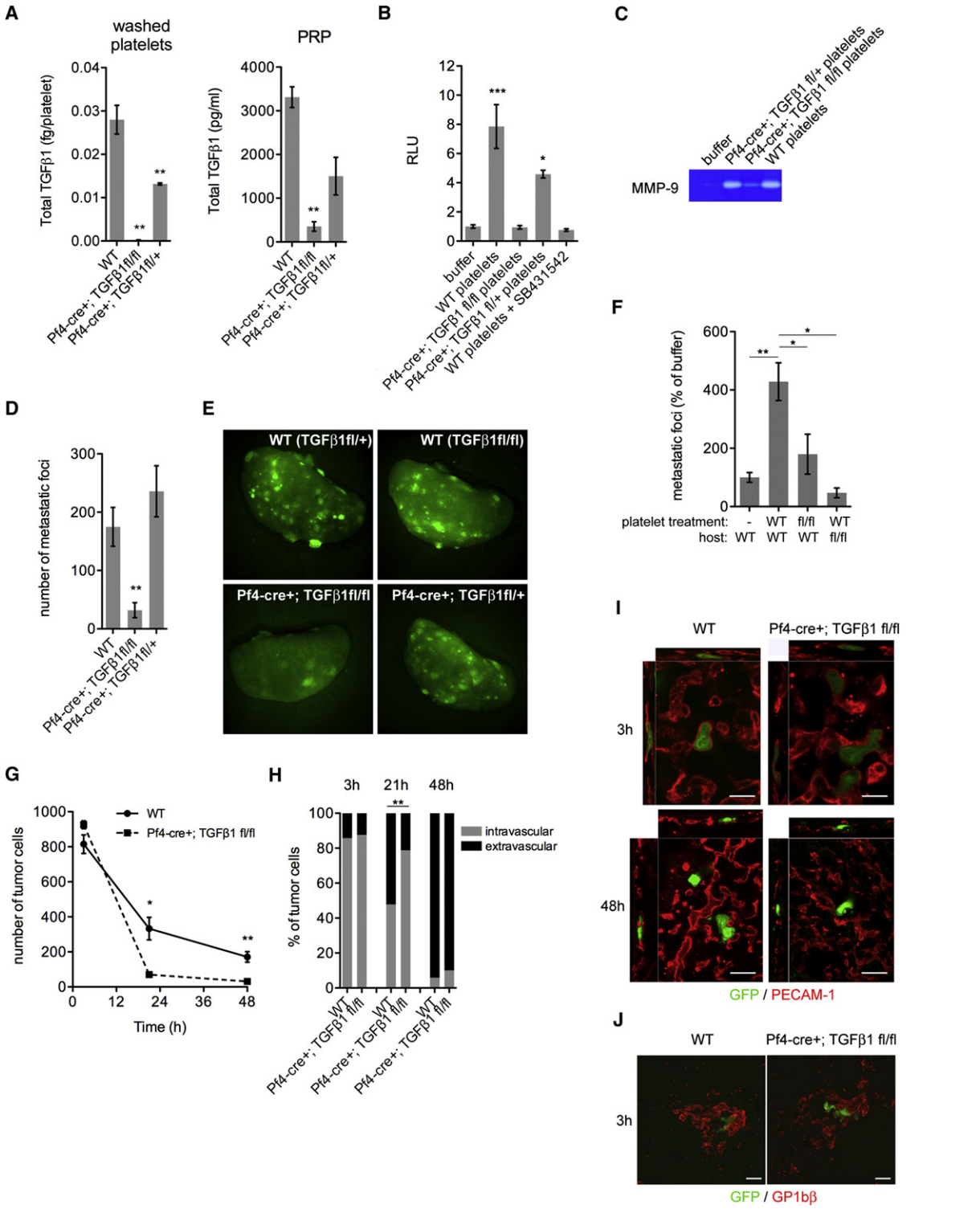

Figure 3. Platelet-Derived TGFβ1 Promotes Lung Metastasis

(A) Concentration of TGFβ1 in washed platelets and platelet-rich plasma (PRP) from WT, *Pf4-cre*$^{+}$*; TGFβ1*$^{fl/fl}$ or *Pf4-cre*$^{+}$*; TGFβ1*$^{fl/+}$ mice measured by ELISA (n = 2). Each bar represents the mean ± SEM, and **p < 0.01 versus WT were determined by one-way ANOVA followed by Tukey's posttest.

(B) Relative luciferase activity (RLU) in Ep5 cells stably expressing a luciferase reporter under the control of the SBE promoter and treated with buffer, platelets from WT, *Pf4-cre*$^{+}$*; TGFβ1*$^{fl/fl}$, or *Pf4-cre*$^{+}$*; TGFβ1*$^{fl/+}$ mice, or with WT platelets + SB431542 (10 μM) for 20 hr (n = 3). Each bar represents the mean ± SEM, and *p < 0.05, ***p < 0.001 versus buffer were determined by one-way ANOVA followed by Tukey's posttest.

(C) Zymography for MMP-9 in the conditioned medium from Ep5 cells treated with buffer, platelets from WT, *Pf4-cre*$^{+}$*; TGFβ1*$^{fl/fl}$ or *Pf4-cre*$^{+}$*; TGFβ1*$^{fl/+}$ mice for 40 hr.

gene signatures are enriched in platelet- or platelet pellet-treated Ep5 cells, but not in platelet releasate-treated cells (Table S4). Importantly, treatment of tumor cells with either TGFβ1-deficient platelets or with WT platelets together with the TGFβRI inhibitor SB431542 still led to activation of the NF-κB pathway reporter (Figure 6C), ruling out the possibility that activation of the NF-κB pathway is TGFβ1-dependent in this context.

To study whether NF-κB signaling contributes to the prometastatic phenotype observed upon platelet contact, we established Ep5 cells stably expressing an IκBα mutant (IκBαS32A/S36A) that cannot be phosphorylated or degraded and therefore irreversibly sequesters NF-κB in the cytoplasm, and inhibits its function (IκBα super-repressor; Ep5-IkBSR) (Brown et al., 1995). In contrast to Ep5 expressing a control vector (Ep5-vector), Ep5-IkBSR cells failed to activate an NF-κB-dependent luciferase reporter and did not express increased levels of MCP-1 following platelet treatment, demonstrating that the NF-κB signaling is blocked in these cells (Figures 6D and 6E). Importantly, pretreatment of Ep5-vector cells with platelets prior to tail-vein injection led to increased numbers of metastases, whereas it failed to enhance metastasis of Ep5-IkBSR cells (Figure 6F). Similarly, retention of Ep5-IkBSR cells in the lungs after 48 hr was not enhanced by a pretreatment with platelets, showing that the NF-κB pathway is necessary for the prometastatic effects of platelets on tumor cells (Figure 6G). Furthermore, Ep5-IkBSR cells did not acquire a mesenchymal morphology (Figure 6H) and did not display increased invasion (Figure 6I) in response to treatment with platelets. These results correlated with lower levels of MMP-9 secretion (Figure 6J) and lower *vimentin* and *fibronectin* gene expression (Figure 6K) by Ep5-IkBSR cells following platelet treatment. The inhibition of platelet prometastatic effects was not due to an impairment of TGFβ/Smad signaling pathway by the IkBSR construct because Smad2 phosphorylation levels were intact in Ep5-IkBSR cells (Figure S4C). In addition, inhibition of MMP-9 secretion and vimentin protein expression induced upon platelet treatment were also observed when Ep5 cells were treated with JSH-23, a pharmacological inhibitor of the NF-κB pathway (Figures S4D and S4E). JSH-23 treatment also abolished the synergy observed on *PAI-1* reporter activity between TGFβ1 and platelets (Figure S4F), but had no effect on SBE-reporter activity (Figure S4G). This finding further demonstrates that platelets activate NF-κB independently of TGFβ/Smad signaling, and cooperate with TGFβ1 to induce an EMT-like transformation in cancer cells. Thus, the ability of platelets to prime tumor cells for metastasis depends on the synergistic interaction between the NF-κB and TGFβ signaling pathways, which is triggered by direct platelet-tumor cell contact (Figure 7).

DISCUSSION

Signals provided by the primary tumor microenvironment are important modulators of the capacity of tumor cells to invade, access the vasculature, and metastasize (Joyce and Pollard, 2009; Nguyen et al., 2009). However, the metastatic potential of tumor cells may be further defined in response to signals provided during their intravascular transit. Here, we have tested this hypothesis and show that platelets present in the bloodstream actively signal to tumor cells to promote their metastatic potential outside of the primary microenvironment. This effect is independent of any direct contribution of platelets to immunosurveillance, adhesion, or physical shielding functions, as tumor cells can be primed for metastasis by a transient exposure to purified platelets in vitro. Mechanistically, a transient contact between platelets and tumor cells is sufficient to induce a prometastatic gene expression signature, induce an EMT-like transformation and invasive behavior in vitro, and promote metastatic seeding in the lungs in vivo (Figure 7). Considering that tumor cells would normally interact with platelets once in the bloodstream, these results suggest that tumor cells could gain a more mesenchymal phenotype and increased metastatic capacities after leaving the primary tumor microenvironment. This implies that cells that have intravasated without losing their epithelial properties either via leaky blood vessels (Carmeliet and Jain, 2000; Mazzone et al., 2009) or via collective invasion mechanisms (Friedl and Gilmour, 2009) could acquire a mesenchymal phenotype during their transit in the vasculature. In support of this idea, circulating tumor cells have been found to express epithelial markers (EpCAM, cytokeratins), suggesting that EMT is not absolutely required to access the blood flow (Nagrath et al., 2007). Thus, interactions with platelets may be particularly important in mediating extravasation of circulating epithelial tumor cells, and to maintain or further enhance the extravasation potential of circulating mesenchymal tumor cells. In this respect, it would be interesting to define the impact of platelets on gene expression and metastatic potential of circulating tumor cells from cancer patients.

Several signaling molecules, including TGFβ, PDGF, VEGF and angiopoietin are abundant in platelets (Erpenbeck and Schön, 2010; Sierko and Wojtukiewicz, 2007) and may therefore

(D and E) Numbers of metastatic foci at the surface of lungs (two largest lobes) 14 days after tail-vein injection of MC38GFP cells in WT, *Pf4-cre*$^{+}$*; TGFβ1*$^{fl/fl}$ or *Pf4-cre*$^{+}$*; TGFβ1*$^{fl/+}$ mice (n = 7–9), and representative pictures of lungs (E). (D) Each bar represents the mean ± SEM, and **p < 0.01 versus WT was determined by one-way ANOVA followed by Tukey's posttest.

(F) Numbers of metastatic foci at the surface of lungs (two largest lobes) 14 days after tail-vein injection of MC38GFP cells pretreated with buffer (−), platelets from WT mice (WT) or platelets from *Pf4-cre*$^{+}$*; TGFβ1*$^{fl/fl}$ (fl/fl) and injected into WT or *Pf4-cre*$^{+}$*; TGFβ1*$^{fl/fl}$ mice (n = 9–14). Each bar represents the mean ± SEM, and *p < 0.05, **p < 0.01 were determined by one-way ANOVA followed by Tukey's posttest.

(G) Numbers of tumor cells at the surface of lungs 3 hr, 21 hr, and 48 hr after tail-vein injection of MC38GFP cells in WT or *Pf4-cre*$^{+}$*; TGFβ1*$^{fl/fl}$ mice. Each point represents the mean ± SEM number of cells/view field (3×) (n = 3–14). *p < 0.05, **p < 0.01 were determined by Student's t test.

(H) Percentage of intravascular and extravascular MC38GFP cells in lungs of WT or *Pf4-cre*$^{+}$*; TGFβ1*$^{fl/fl}$ mice 3 hr, 21 hr, and 48 hr after tail-vein injection of tumor cells (n = 16–46 cells). **p < 0.01 as determined by Fisher's exact test.

(I and J) Confocal microscopy of lungs of WT or *Pf4-cre*$^{+}$*; TGFβ1*$^{fl/fl}$ mice 3 hr and 48 hr after tail-vein injection of tumor cells for MC38GFP cells (green) and either blood vessels (I; PECAM-1 staining; red) or platelets (J; GP1bβ staining; red. Note platelet aggregates surrounding tumor cells.). Scale bar represents 50 μm. See also Figure S2 and Table S3.

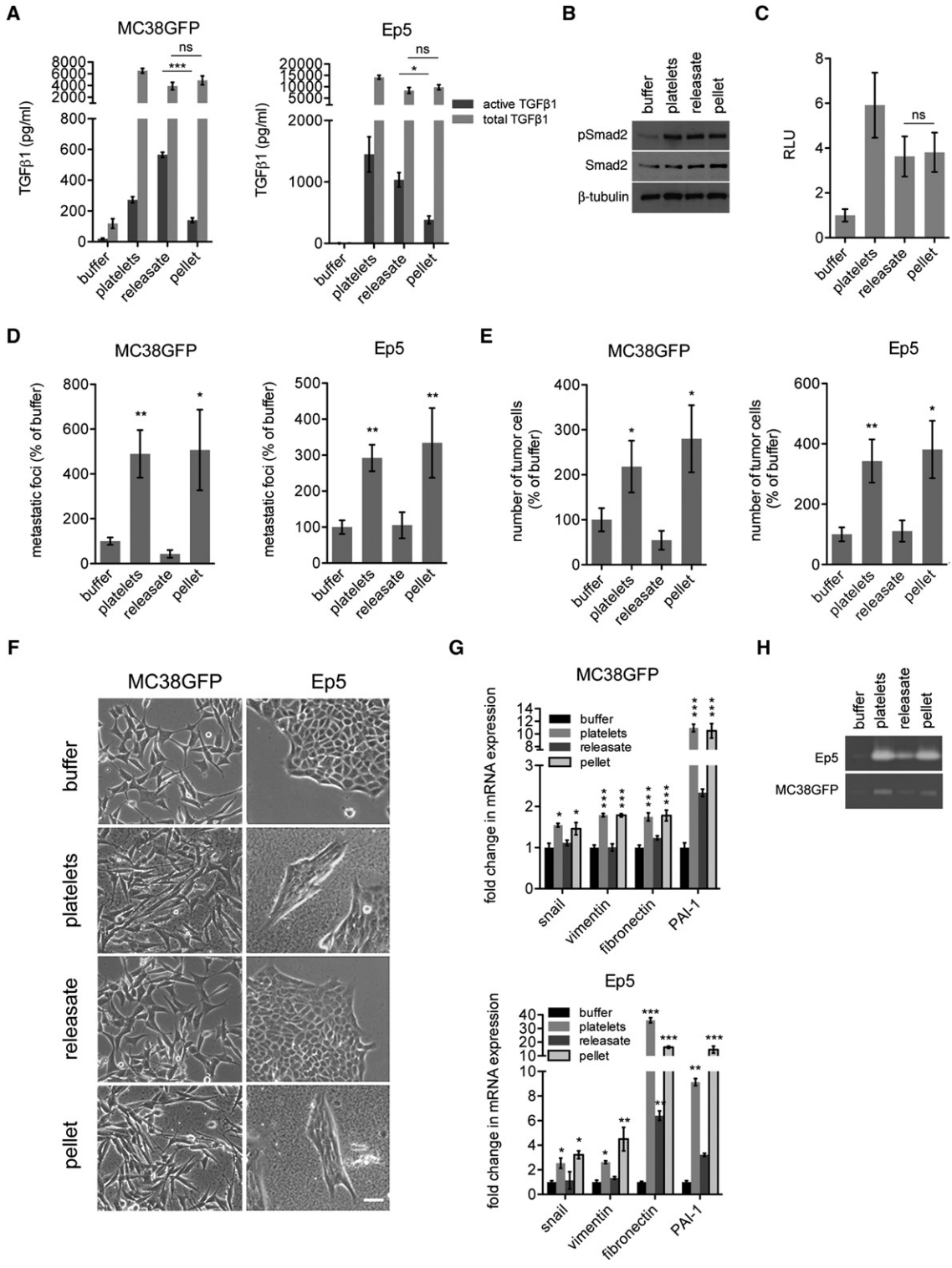

Figure 4. Platelet-Derived TGFβ1 and Platelet-Bound Factors Cooperate to Promote Metastasis

(A) Concentration of TGFβ1 measured by ELISA in the conditioned medium of MC38GFP or Ep5 cells incubated with buffer, platelets, releasate from activated platelets (releasate), or the pellet fraction from activated platelets (pellet) for 40 hr (n = 4–6). Each bar represents the mean ± SEM, and ns ($p > 0.05$), *$p < 0.05$, ***$p < 0.001$ were determined by one-way ANOVA followed by Tukey's posttest.

(B) Detection of phospho-Smad2 and total Smad2 protein levels by immunoblotting in Ep5 cells treated as in (A). β-tubulin was used as loading control.

(C) Relative luciferase activity (RLU) in Ep5 cells stably expressing a luciferase reporter under the control of the SBE promoter and treated as in (A) for 20 hr (n = 2). Each bar represents the mean ± SEM, and ns ($p > 0.05$) was determined by one-way ANOVA followed by Tukey's posttest.

impact tumor cell behavior and induce EMT. Our results show that the prometastatic effects of platelets are in large part mediated via activation of the TGFβ signaling pathway, and that abrogating either TGFβ signaling in tumor cells or TGFβ expression by platelets is sufficient to inhibit metastasis and EMT. Although TGFβ has been implicated in the induction of a prometastatic phenotype in many contexts (Padua et al., 2008; Siegel et al., 2003), the relevant cellular source of TGFβ bioavailable to circulating tumor cells, particularly at the site of metastatic extravasation, was previously unclear.

Our results strongly indicate that platelets are an important source of bioavailable TGFβ for tumor cells in the circulation and at the site of extravasation. This finding is supported by the observation that platelets contain concentrations of TGFβ1 many-fold higher than most cell types (Assoian et al., 1983). Furthermore, the amount of TGFβ1 produced by other cells and taken up by platelets seems minimal, as purified platelets from *Pf4-cre*$^{+}$*; TGFβ1*$^{fl/fl}$ mice contained <1% of the amount of TGFβ1 present in platelets from WT mice.

Most importantly, we show that abrogation of TGFβ1 expression solely in platelets and megakaryocytes is sufficient to inhibit metastasis and prevent the seeding of tumor cells in the lungs. Furthermore, the presence of platelet-derived TGFβ1 in situ in the host bloodstream is crucial for metastasis, because pretreating tumor cells with platelets from WT mice fails to enhance metastasis formation in mice lacking TGFβ1 in their platelets. Because platelet-tumor cell interactions are transient and occur only within the first 24 hr (Läubli et al., 2006 and data not shown), we propose that platelets could provide a pulse of TGFβ1 to circulating tumor cells, which would allow them to gain a more invasive, mesenchymal-like phenotype and extravasate. Along these lines, previous studies have shown that tumor cells transiently exposed to TGFβ1 have an enhanced capacity to seed the lungs, whereas cells that are continuously exposed to TGFβ1 have decreased metastatic capacity due to the cytostatic effect of TGFβ1 (Giampieri et al., 2009; Padua et al., 2008). In this respect, specific therapeutic inhibition of platelet-derived TGFβ1 might result in the impairment of tumor cell extravasation at the metastatic site. Importantly, *Pf4-cre*$^{+}$*; TGFβ1*$^{fl/fl}$ mice maintain normal platelet counts and hemostatic functions, suggesting that pharmacological inhibition of platelet-derived TGFβ could inhibit metastasis without adverse effects on physiological hemostasis.

We also find that, although required for metastasis, activation of TGFβ signaling alone is unable to generate effects of the magnitude of those observed with platelets. Indeed, although tumor cells treated for 24 hr with platelets or with the pellet fraction from activated platelets undergo EMT, cells treated with the releasate of activated platelets (that contained a similar concentration of TGFβ1) do not. In line with this result, a prolonged treatment with TGFβ1—typically 1 week or longer—is needed to induce EMT in several epithelial cancer cell lines including Ep5 cells (Labelle et al., 2008; Mani et al., 2008; Maschler et al., 2005). Our data further support the existence of additional platelet-bound factors synergizing with TGFβ1. First, platelets induce the TGFβ-responsive *PAI-1* reporter to levels higher than achievable with TGFβ1 alone. Second, combining exogenous TGFβ1 with platelets from either WT or *Pf4-cre*$^{+}$*; TGFβ1*$^{fl/fl}$ mice results in a synergistic activation of the *PAI-1* reporter. Last, the synergistic effects on *PAI-1* reporter activity as well as the induction of prometastatic genes are blocked if platelets are separated from tumor cells by a semipermeable membrane. Thus, our results clearly demonstrate that additional platelet-bound factors synergize with TGFβ1 to promote metastasis, and to induce a prometastatic EMT program in tumor cells. In particular, we show that this synergy is dependent on the activation of the NF-κB pathway, which is specifically triggered upon direct contact between tumor cells and platelets independently from TGFβ activity.

NF-κB regulates the expression of proinflammatory genes and has been associated with increased metastasis and EMT induction (Huber et al., 2004; Lin and Karin, 2007). For example, NF-κB promotes osteolytic bone metastasis by inducing the proinflammatory cytokine GM-CSF (Park et al., 2007). Notably, the activation of NF-κB has also been proposed to be part of the mechanism allowing TGFβ signaling to switch from a cytostatic to a prometastatic signal (Neil and Schiemann, 2008). In support of this idea, we found that NF-κB activation potentiates TGFβ-induced prometastatic gene expression, and that NF-κB signaling is necessary for the induction of EMT and efficient metastatic seeding upon platelet-cancer cell interactions. Thus, platelet-tumor cell contacts during metastasis potentiate tumor cell transcriptional responses to TGFβ via NF-κB activation.

In conclusion, we establish platelets as a crucial source of TGFβ bioavailable to tumor cells in the vasculature and necessary for tumor cell extravasation and metastasis formation. Importantly, our study reveals that platelets are more than physical shields and actively signal to tumor cells via the TGFβ and NF-κB pathways to potently induce a prometastatic phenotype. We thus propose a model whereby the metastatic potential of tumor cells continues to evolve outside of the primary tumor site, in response to tumor-host interactions in the bloodstream and at the site of metastasis. In particular, we identify platelet-tumor cell interactions and the signaling pathways that they trigger as fundamental determinants of cancer metastasis that may provide the basis for developing effective anti-metastatic therapies.

(D) Numbers of metastatic foci at the surface of lungs (two largest lobes) 14 days after tail-vein injection of MC38GFP or Ep5-ZsGreen cells pretreated with buffer, platelets, releasate from activated platelets (releasate), or the pellet fraction from activated platelets (pellet) for 40 hr (n = 5–17). Each bar represents the mean ± SEM, and *p < 0.05, **p < 0.01 versus buffer were determined by one-way ANOVA followed by Tukey's posttest.
(E) Numbers of tumor cells at the surface of lungs 48h after tail-vein injection of MC38GFP or Ep5-ZsGreen cells pretreated as in (D). Each bar represents the mean ± SEM number of cells/view field (3×) (n = 5–13). *p < 0.05, **p < 0.01 versus buffer were determined by Student's t test.
(F) Phase-contrast micrographs of MC38GFP and Ep5 cells treated as in (A) for 24 hr. Scale bar represents 50 μm.
(G) Relative fold change in mRNA expression in MC38GFP or Ep5 cells treated as in (A) for 40 hr. Values are normalized to *Gapdh* expression (n = 3). Each bar represents the mean ± SEM, and *p < 0.05, **p < 0.01, ***p < 0.001 versus buffer were determined by one-way ANOVA followed by Tukey's posttest.
(H) Zymography for MMP-9 in the conditioned medium from Ep5 or MC38GFP cells treated as in (A) for 40 hr. See also Figure S3 and Table S4.

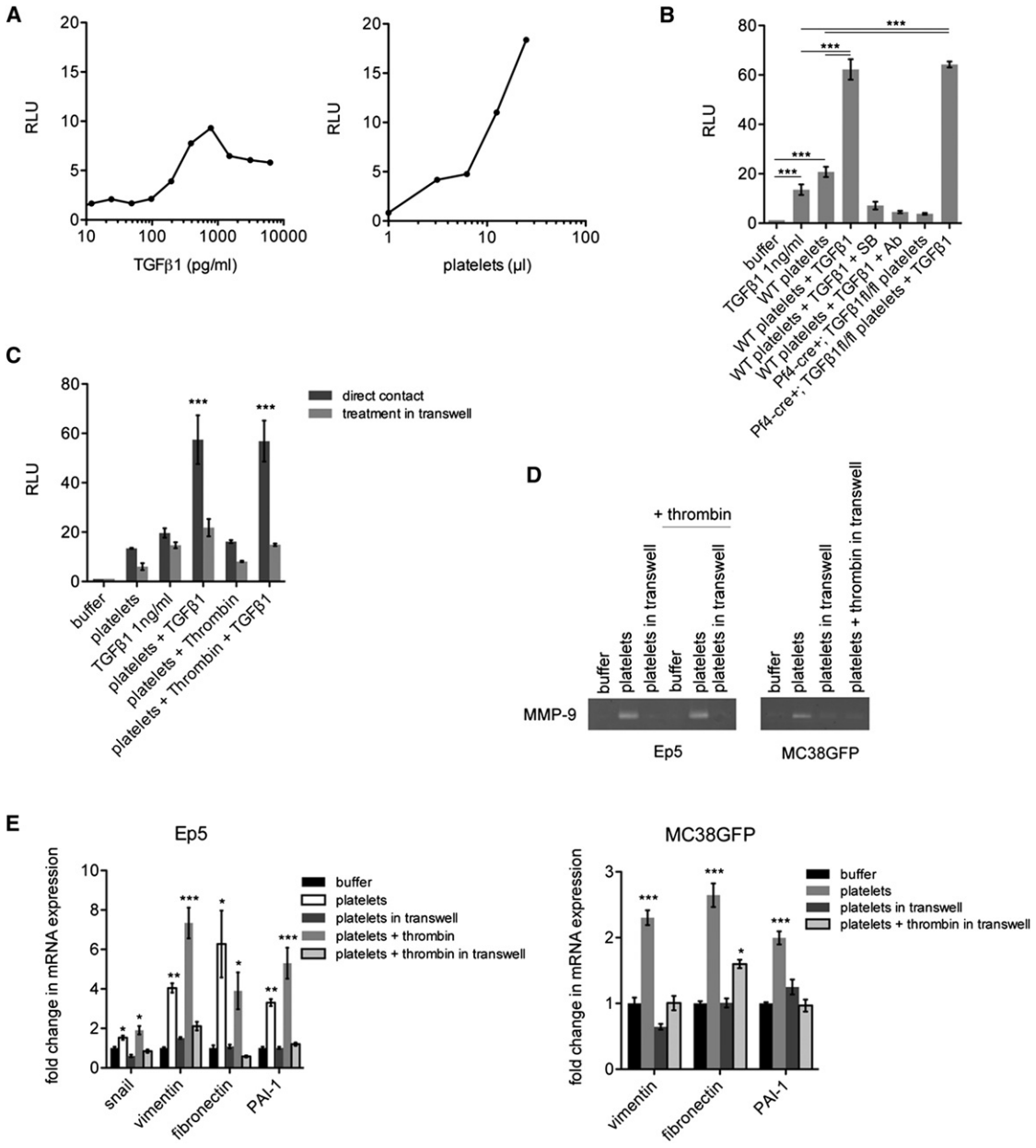

Figure 5. TGFβ1 and Direct Platelet-Tumor Cell Contact Synergize to Promote Prometastatic Gene Expression

(A) Relative luciferase activity (RLU) in MLEC cells stably expressing a luciferase reporter under the control of a TGFβ responsive *PAI-1* promoter construct and treated with different concentrations of TGFβ1 (left) or platelets (right). Note that the y axis scale is the same for both panels and that platelets give higher stimulation than achievable with TGFβ1 alone.

(B) Relative luciferase activity (RLU) in MLEC cells stably expressing a luciferase reporter under the control of a *PAI-1* promoter construct treated with buffer, platelets from WT or *Pf4-cre*$^{+}$*; TGFβ1*$^{fl/fl}$ mice, TGFβ1 (1 ng/ml) or with combinations of platelets + TGFβ1 (1 ng/ml), +/− SB431542 (SB; 10 μM) or +/− TGFβ1 blocking antibody (Ab; 6 μg/ml)(n = 3–16). Each bar represents the mean ± SEM, and ***p < 0.001 were determined by one-way ANOVA followed by Tukey's posttest.

(C) Relative luciferase activity (RLU) in MLEC cells stably expressing a luciferase reporter under the control of a *PAI-1* promoter construct treated with buffer, platelets, or thrombin-activated platelets +/− TGFβ1 (1ng/ml) seeded either at the bottom (direct contact with tumor cells) or in the upper chamber of a transwell (0.4 μm pore size) to prevent direct contact between platelets and tumor cells (n = 2–3). Each bar represents the mean ± SEM, and ***p < 0.001 versus buffer were determined by one-way ANOVA followed by Tukey's posttest.

(D) Zymography for MMP-9 in the conditioned medium from Ep5 or MC38GFP cells treated with buffer, platelets, or thrombin-activated platelets seeded either at the bottom or in the upper chamber of a transwell (0.4 μm pore size).

(E) Relative fold change in mRNA expression in Ep5 or MC38GFP cells treated as in (D) (n = 3). Values are normalized to *Gapdh* expression. Each bar represents the mean ± SEM, and *p < 0.05, **p < 0.01, ***p < 0.001 versus buffer were determined by one-way ANOVA followed by Tukey's posttest.

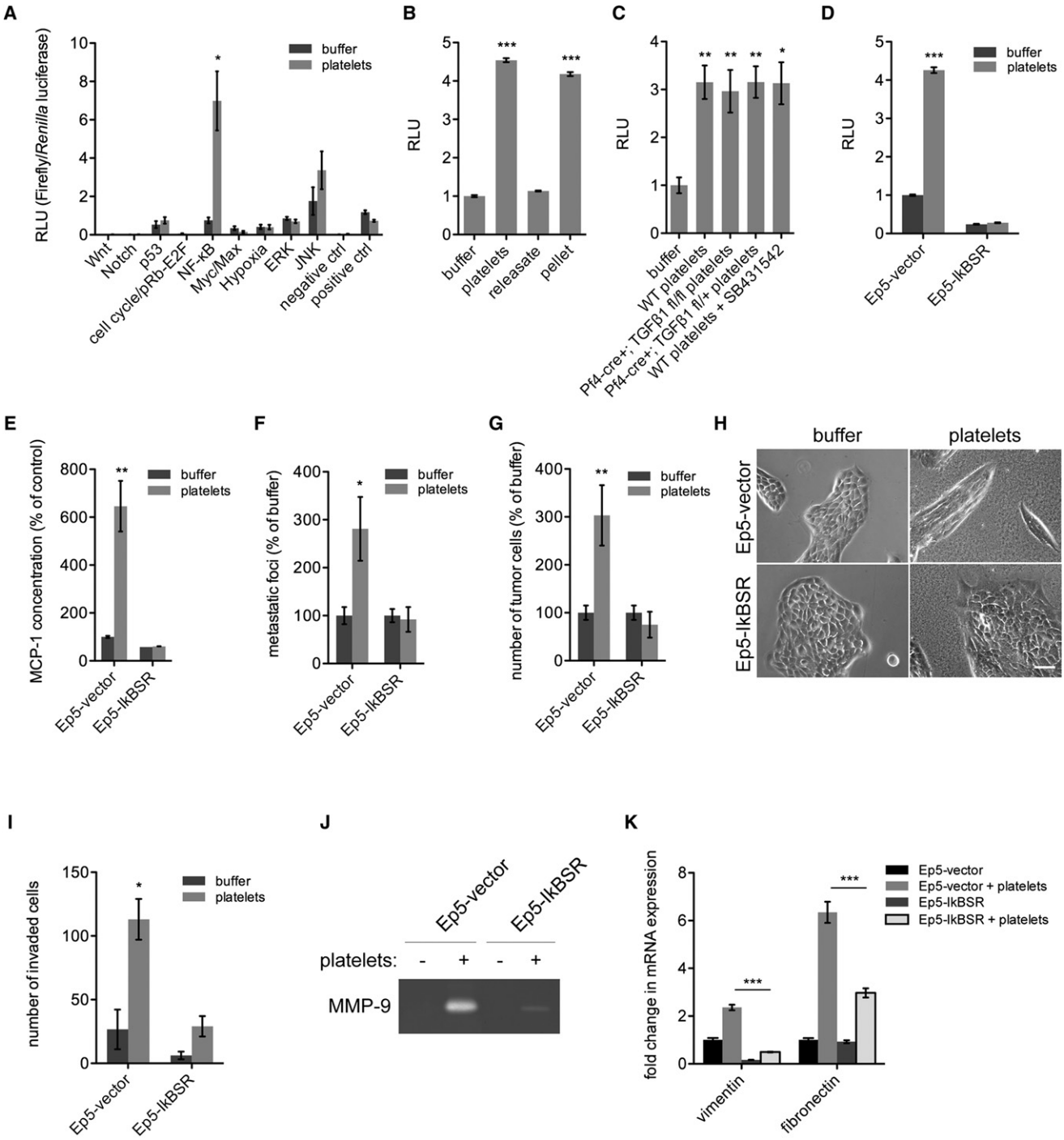

Figure 6. The NF-κB Signaling Pathway Is Activated by Platelets in a Contact-Dependent Manner and Cooperates with TGFβ Signaling to Induce an EMT-Like Transition and Promote Metastasis

(A) Ep5 cells were transfected with pathway-specific firefly luciferase reporters and constitutively expressed control *Renilla* luciferase reporters. Twenty-four hours after transfection, cells were treated with buffer or platelets for 20 hr, and the relative luciferase activity (RLU) was measured. Firefly luciferase activity was normalized to *Renilla* luciferase activity. Each bar represents the mean ± SEM of n = 3. *p < 0.05 was determined by Student's t test.

(B) Relative luciferase activity (RLU) in Ep5 cells stably expressing an NF-κB luciferase reporter and treated with buffer, platelets, releasate from activated platelets (releasate), or the pellet fraction from activated platelets (pellet) for 20 hr (n = 2). Each bar represents the mean ± SEM, and ***p < 0.001 versus buffer were determined by one-way ANOVA followed by Tukey's posttest.

(C) Relative luciferase activity (RLU) in Ep5 cells stably expressing a NF-κB luciferase reporter and treated with buffer, platelets from WT, *Pf4-cre*$^{+}$*; TGFβ1*$^{fl/fl}$, or *Pf4-cre*$^{+}$*; TGFβ1*$^{fl/+}$ mice, or with WT platelets + SB431542 (10 μM) for 20 hr (n = 5). Each bar represents the mean ± SEM, and *p < 0.05, **p < 0.01 versus buffer were determined by one-way ANOVA followed by Tukey's posttest.

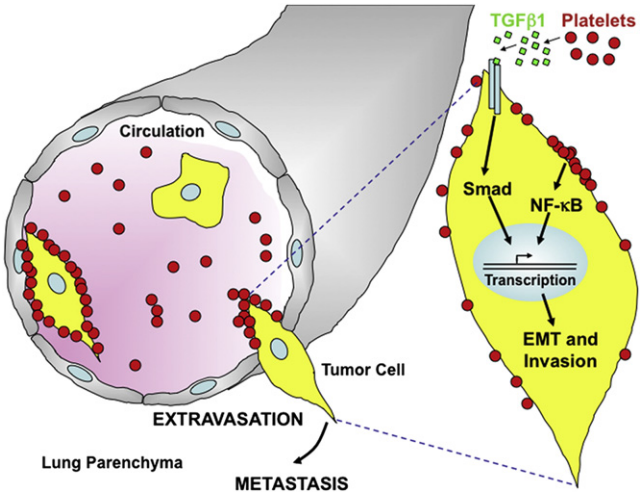

Figure 7. Platelet-Tumor Cell Contact and Platelet-Derived TGFβ1 Synergize to Promote an EMT-Like Transition and Metastasis

Platelets secrete TGFβ1, which activates the TGFβ/Smad pathway in tumor cells. Upon direct platelet-tumor cell contact, the NF-κB pathway is also activated in tumor cells and synergizes with TGFβ/Smad signaling to induce a rapid EMT, enhance invasiveness and promote metastasis. Activation of neither the TGFβ/Smad nor the NF-κB pathway alone is sufficient to promote metastasis. Thus, platelet-tumor cell contact triggers a synergistic interaction between TGFβ/Smad and NF-κB pathways that is necessary for efficient metastasis. The metastatic potential of tumor cells therefore continues to evolve outside of the primary tumor site in response to platelet-to-tumor cell signaling.

EXPERIMENTAL PROCEDURES

Mice

Mice homozygous for the *TGFβ1* floxed allele (*TGFβ1*$^{fl/fl}$; obtained from R. Flavell) (Li et al., 2007) on a C57BL/6 genetic background were crossed with *Pf4-cre* mice on a C57BL/6 background (obtained from S. Shattil) (Tiedt et al., 2007). To obtain mice with TGFβ1-deficient platelets, *Pf4-cre*$^{+}$*; TGFβ1*$^{fl/+}$ mice were bred with *TGFβ1*$^{fl/fl}$ or *TGFβ1*$^{fl/+}$ mice. *TGFβ1*$^{+/-}$ mice (the null allele was obtained by *egfp* knockin, which disrupted *TGFβ1* without affecting *stumpy*) (Li et al., 2007) were crossed with *Pf4-cre*$^{+}$*; TGFβ1*$^{fl/fl}$ mice to obtain *Pf4-cre*$^{+}$*; TGFβ1*$^{fl/-}$ mice. For genotyping primers, see Supplemental Experimental Procedures. All mice were housed and handled in accordance with approved Massachusetts Institute of Technology Division of Comparative Medicine protocols.

Generation of Cell Lines Stably Expressing ZsGreen, IkBSR, and Luciferase-Based Reporters

Retroviral vectors coding for ZsGreen or IκBα super-repressor plus GFP (IkBSR) were transduced into Ep5 cells as described previously (Stern et al., 2008) and in Supplemental Experimental Procedures. Ep5 and MC38GFP cell lines stably expressing SBE (AGCCAGACA tandem repeats)-luciferase and NF-κB (GGGACTTTCC tandem repeats)-luciferase reporter constructs were generated by infecting cells with Cignal Lenti Reporter vectors (SABiosciences) according to manufacturers' instructions.

Preparation of Platelets and Platelet Fractions

Mouse blood was collected by cardiac puncture and washed platelets were prepared as described previously (Frenette et al., 1995; Hartwell et al., 1998). To prepare platelet fractions, platelets were activated with thrombin 0.5 U/ml for 15 min at 37°C. The pellet fraction was separated from the releasate (supernatant) by centrifugation at 2800 × g for 7 min.

Treatment of Tumor Cells with Platelets

Cells were seeded in DMEM 10% FCS and incubated overnight. Immediately prior to treatment the medium was changed for fresh DMEM. A total of 150,000 platelets/μl and equivalent volumes of releasate and pellet fractions were added. Where indicated, cells were treated with 1 or 10 ng/ml of recombinant TGFβ1 (R&D Systems), 10 μM SB431542 (Sigma), or 6 μg/ml anti-TGFβ1 blocking antibody (R&D systems).

In Vivo Metastasis Assays

For lung metastasis assays, cells treated with platelets for 40 hr were washed in PBS, and either trypsinized (Ep5) or lifted with 2mM EDTA in PBS (MC38GFP). Cells were then washed and centrifuged twice to remove platelets, and resuspended in HBSS at a constant number of cells for all mice in a given experiment (250,000 to 1,000,000 cells/injection). One hundred microliters of cell suspension were then injected via the tail vein of syngeneic mice. The numbers of single cells and metastatic foci were determined as described in Supplemental Experimental Procedures.

Microarray Analysis

Total RNA was isolated from platelet-treated or untreated Ep5 cells (n = 5). In order to detect mRNAs contributed by platelets, RNA was also isolated from platelet lysates mixed with untreated Ep5 cells lysates immediately prior to RNA isolation (n = 3) (the concentration of RNA isolated from platelets alone was below detection limits and could therefore not be used for microarray analysis). cRNA was then synthesized and hybridized onto GeneChip Mouse Exon 1.0 ST Arrays (Affymetrix).

Luciferase Assay

A total of 15,000 Ep5 cells/50 μl Opti-MEM were plated in a 96-well Cignal Finder Multi Pathway reporter Array plate as recommended by the manufacturer (SABiosciences) and incubated for 24 hr. The medium was

(D) Relative luciferase activity (RLU) in Ep5 cells stably expressing a NF-κB luciferase reporter and either a IκB super-repressor (Ep5-IkBSR) or a control vector (Ep5-vector) and treated with buffer or platelets for 20 hr (n = 4). Each bar represents the mean ± SEM, and ***p < 0.001 versus buffer was determined by two-way ANOVA followed by Bonferroni's posttest.

(E) MCP-1 concentration in the conditioned medium from Ep5 cells stably expressing an IκB super-repressor (Ep5-IkBSR) or a control vector (Ep5-vector) and treated with buffer or platelets for 20 hr (n = 2). Each bar represents the mean ± SEM, and **p < 0.01 versus buffer was determined by two-way ANOVA followed by Bonferroni's posttest.

(F) Numbers of metastatic foci at the surface of lungs (two largest lobes) 14 days after tail-vein injection of Ep5-IkBSR and Ep5-vector cells pretreated with buffer or platelets for 40h. Each bar represents the mean ± SEM of n = 5–7. *p < 0.05 was determined by Student's t test.

(G) Numbers of tumor cells at the surface of lungs 48 hr after tail-vein injection of Ep5-IkBSR and Ep5-vector cells pretreated with buffer or platelets for 40 hr. Each bar represents the mean ± SEM of n = 4–7. **p < 0.01 was determined by Student's t test.

(H) Phase-contrast micrographs of Ep5-IkBSR and Ep5-vector cells treated with buffer or platelets for 24 hr. Scale bar represents 50 μm.

(I) Ep5-IkBSR and Ep5-vector cells were added at the top of transwells coated with Matrigel and treated with buffer or platelets. The total numbers of cells that invaded to the bottom of the transwell were counted after 48 hr (n = 2). Each bar represents the mean ± SEM, and *p < 0.05 versus buffer was determined by two-way ANOVA followed by Bonferroni's posttest.

(J) Zymography for MMP-9 in the conditioned medium from Ep5-IkBSR and Ep5-vector cells treated with buffer or platelets for 40 hr.

(K) Relative fold change in mRNA expression in Ep5-IkBSR and Ep5-vector cells treated as in (J) (n = 3). Values are normalized to *Gapdh* expression. Each bar represents the mean ± SEM, and ***p < 0.001 were determined by one-way ANOVA followed by Tukey's posttest. See also Figure S4.

then changed and cells were treated with platelets or platelet fractions. The ratios of Firefly to *Renilla* Luciferase activities (relative light units [RLU]) were measured in cell lysates with the Dual Luciferase Reporter Assay System (Promega) 24 hr after treatment with platelets.

TGFβ1 ELISA

TGFβ1 levels were detected in tissue-culture-conditioned medium (40 hr), washed platelets or platelet-rich plasma either by direct assay (active TGFβ1), or following acid treatment to activate latent TGFβ1 (total TGFβ1) with the Quantikine TGFβ1 immunoassay kit (R&D Systems).

MCP-1 Detection

Concentration of MCP-1 in conditioned medium of Ep5 or MC38GFP cells was analyzed with CBA soluble Flex Set cytometric beads, following manufacturer's instructions (BD Biosciences).

Statistics

Statistical analyses were performed with the GraphPad Prism Software following guidelines found in Bremer and Doerge (2010) and in GraphPad Prism. Briefly, the Student's t test was used to compare means of two independent groups to each other, whereas one-way ANOVA followed by Tukey's posttest was used to compare the means of more than two independent groups. Two-way ANOVA followed by Bonferroni's posttest was used to compare the means of groups influenced by two independent factors.

ACCESSION NUMBERS

Microarray data are deposited in Gene Expression Omnibus under accession number GSE27456.

SUPPLEMENTAL INFORMATION

Supplemental Information includes four figures, four tables, and Supplemental Experimental Procedures and can be found with this article online at doi:10.1016/j.ccr.2011.09.009.

ACKNOWLEDGMENTS

We are grateful to Patrick Stern for viral vectors driving ZsGreen and IkBSR expression, and to Richard Flavell and Sanford Shattil for mouse strains. We thank Charlie Whittaker (Swanson Biotechnology Center, Koch Institute) for assistance with microarray analysis, members of the Hynes lab for advice, and John Lamar and Patrick Stern for critically reading the manuscript. This work was supported by the Ludwig Center for Molecular Oncology at MIT, by the Koch Institute at MIT, and by the Howard Hughes Medical Institute of which R.O.H. is an Investigator. M.L. was supported by a postdoctoral fellowship from the Anna Fuller Fund.

Received: February 21, 2011
Revised: June 28, 2011
Accepted: September 20, 2011
Published: November 14, 2011

REFERENCES

Abe, M., Harpel, J.G., Metz, C.N., Nunes, I., Loskutoff, D.J., and Rifkin, D.B. (1994). An assay for transforming growth factor-beta using cells transfected with a plasminogen activator inhibitor-1 promoter-luciferase construct. Anal. Biochem. *216*, 276–284.

Assoian, R.K., and Sporn, M.B. (1986). Type beta transforming growth factor in human platelets: release during platelet degranulation and action on vascular smooth muscle cells. J. Cell Biol. *102*, 1217–1223.

Assoian, R.K., Komoriya, A., Meyers, C.A., Miller, D.M., and Sporn, M.B. (1983). Transforming growth factor-beta in human platelets. Identification of a major storage site, purification, and characterization. J. Biol. Chem. *258*, 7155–7160.

Bakewell, S.J., Nestor, P., Prasad, S., Tomasson, M.H., Dowland, N., Mehrotra, M., Scarborough, R., Kanter, J., Abe, K., Phillips, D., and Weilbaecher, K.N. (2003). Platelet and osteoclast beta3 integrins are critical for bone metastasis. Proc. Natl. Acad. Sci. USA *100*, 14205–14210.

Biswas, S., Guix, M., Rinehart, C., Dugger, T.C., Chytil, A., Moses, H.L., Freeman, M.L., and Arteaga, C.L. (2007). Inhibition of TGF-beta with neutralizing antibodies prevents radiation-induced acceleration of metastatic cancer progression. J. Clin. Invest. *117*, 1305–1313.

Bremer, M., and Doerge, R.W. (2010). Statistics at the Bench: A Step-by Step Handbook for Biologists (Cold Spring Harbor: Cold Spring Harbor Laboratory Press).

Brown, K., Gerstberger, S., Carlson, L., Franzoso, G., and Siebenlist, U. (1995). Control of I kappa B-alpha proteolysis by site-specific, signal-induced phosphorylation. Science *267*, 1485–1488.

Camerer, E., Qazi, A.A., Duong, D.N., Cornelissen, I., Advincula, R., and Coughlin, S.R. (2004). Platelets, protease-activated receptors, and fibrinogen in hematogenous metastasis. Blood *104*, 397–401.

Carmeliet, P., and Jain, R.K. (2000). Angiogenesis in cancer and other diseases. Nature *407*, 249–257.

Corbett, T.H., Griswold, D.P., Jr., Roberts, B.J., Peckham, J.C., and Schabel, F.M., Jr. (1975). Tumor induction relationships in development of transplantable cancers of the colon in mice for chemotherapy assays, with a note on carcinogen structure. Cancer Res. *35*, 2434–2439.

Derynck, R., and Akhurst, R.J. (2007). Differentiation plasticity regulated by TGF-beta family proteins in development and disease. Nat. Cell Biol. *9*, 1000–1004.

Erpenbeck, L., and Schön, M.P. (2010). Deadly allies: the fatal interplay between platelets and metastasizing cancer cells. Blood *115*, 3427–3436.

Frenette, P.S., Johnson, R.C., Hynes, R.O., and Wagner, D.D. (1995). Platelets roll on stimulated endothelium in vivo: an interaction mediated by endothelial P-selectin. Proc. Natl. Acad. Sci. USA *92*, 7450–7454.

Friedl, P., and Gilmour, D. (2009). Collective cell migration in morphogenesis, regeneration and cancer. Nat. Rev. Mol. Cell Biol. *10*, 445–457.

Gasic, G.J., Gasic, T.B., and Stewart, C.C. (1968). Antimetastatic effects associated with platelet reduction. Proc. Natl. Acad. Sci. USA *61*, 46–52.

Gay, L.J., and Felding-Habermann, B. (2011). Contribution of platelets to tumour metastasis. Nat. Rev. Cancer *11*, 123–134.

Giampieri, S., Manning, C., Hooper, S., Jones, L., Hill, C.S., and Sahai, E. (2009). Localized and reversible TGFbeta signalling switches breast cancer cells from cohesive to single cell motility. Nat. Cell Biol. *11*, 1287–1296.

Hartwell, D.W., Mayadas, T.N., Berger, G., Frenette, P.S., Rayburn, H., Hynes, R.O., and Wagner, D.D. (1998). Role of P-selectin cytoplasmic domain in granular targeting in vivo and in early inflammatory responses. J. Cell Biol. *143*, 1129–1141.

Huber, M.A., Azoitei, N., Baumann, B., Grünert, S., Sommer, A., Pehamberger, H., Kraut, N., Beug, H., and Wirth, T. (2004). NF-kappaB is essential for epithelial-mesenchymal transition and metastasis in a model of breast cancer progression. J. Clin. Invest. *114*, 569–581.

Im, J.H., Fu, W., Wang, H., Bhatia, S.K., Hammer, D.A., Kowalska, M.A., and Muschel, R.J. (2004). Coagulation facilitates tumor cell spreading in the pulmonary vasculature during early metastatic colony formation. Cancer Res. *64*, 8613–8619.

Jain, S., Zuka, M., Liu, J., Russell, S., Dent, J., Guerrero, J.A., Forsyth, J., Maruszak, B., Gartner, T.K., Felding-Habermann, B., and Ware, J. (2007). Platelet glycoprotein Ib alpha supports experimental lung metastasis. Proc. Natl. Acad. Sci. USA *104*, 9024–9028.

Joyce, J.A., and Pollard, J.W. (2009). Microenvironmental regulation of metastasis. Nat. Rev. Cancer *9*, 239–252.

Kang, Y., He, W., Tulley, S., Gupta, G.P., Serganova, I., Chen, C.R., Manova-Todorova, K., Blasberg, R., Gerald, W.L., and Massagué, J. (2005). Breast cancer bone metastasis mediated by the Smad tumor suppressor pathway. Proc. Natl. Acad. Sci. USA *102*, 13909–13914.

Karpatkin, S., Pearlstein, E., Ambrogio, C., and Coller, B.S. (1988). Role of adhesive proteins in platelet tumor interaction in vitro and metastasis formation in vivo. J. Clin. Invest. *81*, 1012–1019.

Kim, Y.J., Borsig, L., Varki, N.M., and Varki, A. (1998). P-selectin deficiency attenuates tumor growth and metastasis. Proc. Natl. Acad. Sci. USA *95*, 9325–9330.

Labelle, M., Schnittler, H.J., Aust, D.E., Friedrich, K., Baretton, G., Vestweber, D., and Breier, G. (2008). Vascular endothelial cadherin promotes breast cancer progression via transforming growth factor beta signaling. Cancer Res. *68*, 1388–1397.

Läubli, H., Stevenson, J.L., Varki, A., Varki, N.M., and Borsig, L. (2006). L-selectin facilitation of metastasis involves temporal induction of Fut7-dependent ligands at sites of tumor cell arrest. Cancer Res. *66*, 1536–1542.

Li, M.O., Wan, Y.Y., and Flavell, R.A. (2007). T cell-produced transforming growth factor-beta1 controls T cell tolerance and regulates Th1- and Th17-cell differentiation. Immunity *26*, 579–591.

Lin, W.W., and Karin, M. (2007). A cytokine-mediated link between innate immunity, inflammation, and cancer. J. Clin. Invest. *117*, 1175–1183.

Mani, S.A., Guo, W., Liao, M.J., Eaton, E.N., Ayyanan, A., Zhou, A.Y., Brooks, M., Reinhard, F., Zhang, C.C., Shipitsin, M., et al. (2008). The epithelial-mesenchymal transition generates cells with properties of stem cells. Cell *133*, 704–715.

Maschler, S., Wirl, G., Spring, H., Bredow, D.V., Sordat, I., Beug, H., and Reichmann, E. (2005). Tumor cell invasiveness correlates with changes in integrin expression and localization. Oncogene *24*, 2032–2041.

Mazzone, M., Dettori, D., Leite de Oliveira, R., Loges, S., Schmidt, T., Jonckx, B., Tian, Y.M., Lanahan, A.A., Pollard, P., Ruiz de Almodovar, C., et al. (2009). Heterozygous deficiency of PHD2 restores tumor oxygenation and inhibits metastasis via endothelial normalization. Cell *136*, 839–851.

Nagrath, S., Sequist, L.V., Maheswaran, S., Bell, D.W., Irimia, D., Ulkus, L., Smith, M.R., Kwak, E.L., Digumarthy, S., Muzikansky, A., et al. (2007). Isolation of rare circulating tumour cells in cancer patients by microchip technology. Nature *450*, 1235–1239.

Neil, J.R., and Schiemann, W.P. (2008). Altered TAB1:I kappaB kinase interaction promotes transforming growth factor beta-mediated nuclear factor-kappaB activation during breast cancer progression. Cancer Res. *68*, 1462–1470.

Nguyen, D.X., Bos, P.D., and Massagué, J. (2009). Metastasis: from dissemination to organ-specific colonization. Nat. Rev. Cancer *9*, 274–284.

Nieswandt, B., Hafner, M., Echtenacher, B., and Männel, D.N. (1999). Lysis of tumor cells by natural killer cells in mice is impeded by platelets. Cancer Res. *59*, 1295–1300.

Oft, M., Heider, K.H., and Beug, H. (1998). TGFbeta signaling is necessary for carcinoma cell invasiveness and metastasis. Curr. Biol. *8*, 1243–1252.

Oft, M., Peli, J., Rudaz, C., Schwarz, H., Beug, H., and Reichmann, E. (1996). TGF-beta1 and Ha-Ras collaborate in modulating the phenotypic plasticity and invasiveness of epithelial tumor cells. Genes Dev. *10*, 2462–2477.

Padua, D., Zhang, X.H., Wang, Q., Nadal, C., Gerald, W.L., Gomis, R.R., and Massagué, J. (2008). TGFbeta primes breast tumors for lung metastasis seeding through angiopoietin-like 4. Cell *133*, 66–77.

Palumbo, J.S., Talmage, K.E., Massari, J.V., La Jeunesse, C.M., Flick, M.J., Kombrinck, K.W., Jirousková, M., and Degen, J.L. (2005). Platelets and fibrin(ogen) increase metastatic potential by impeding natural killer cell-mediated elimination of tumor cells. Blood *105*, 178–185.

Park, B.K., Zhang, H., Zeng, Q., Dai, J., Keller, E.T., Giordano, T., Gu, K., Shah, V., Pei, L., Zarbo, R.J., et al. (2007). NF-kappaB in breast cancer cells promotes osteolytic bone metastasis by inducing osteoclastogenesis via GM-CSF. Nat. Med. *13*, 62–69.

Scheel, C., Onder, T., Karnoub, A., and Weinberg, R.A. (2007). Adaptation versus selection: the origins of metastatic behavior. Cancer Res. *67*, 11476–11479, discussion 11479–11480.

Siegel, P.M., Shu, W., Cardiff, R.D., Muller, W.J., and Massagué, J. (2003). Transforming growth factor beta signaling impairs Neu-induced mammary tumorigenesis while promoting pulmonary metastasis. Proc. Natl. Acad. Sci. USA *100*, 8430–8435.

Sierko, E., and Wojtukiewicz, M.Z. (2007). Inhibition of platelet function: does it offer a chance of better cancer progression control? Semin. Thromb. Hemost. *33*, 712–721.

Stern, P., Astrof, S., Erkeland, S.J., Schustak, J., Sharp, P.A., and Hynes, R.O. (2008). A system for Cre-regulated RNA interference in vivo. Proc. Natl. Acad. Sci. USA *105*, 13895–13900.

Thiery, J.P. (2002). Epithelial-mesenchymal transitions in tumour progression. Nat. Rev. Cancer *2*, 442–454.

Tiedt, R., Schomber, T., Hao-Shen, H., and Skoda, R.C. (2007). Pf4-Cre transgenic mice allow the generation of lineage-restricted gene knockouts for studying megakaryocyte and platelet function in vivo. Blood *109*, 1503–1506.

Town, T., Breunig, J.J., Sarkisian, M.R., Spilianakis, C., Ayoub, A.E., Liu, X., Ferrandino, A.F., Gallagher, A.R., Li, M.O., Rakic, P., and Flavell, R.A. (2008). The stumpy gene is required for mammalian ciliogenesis. Proc. Natl. Acad. Sci. USA *105*, 2853–2858.

Yin, J.J., Selander, K., Chirgwin, J.M., Dallas, M., Grubbs, B.G., Wieser, R., Massagué, J., Mundy, G.R., and Guise, T.A. (1999). TGF-beta signaling blockade inhibits PTHrP secretion by breast cancer cells and bone metastases development. J. Clin. Invest. *103*, 197–206.

Cancer Cell, *20*

Supplemental Information

Direct Signaling between Platelets and Cancer Cells Induces an Epithelial-Mesenchymal-Like Transition and Promotes Metastasis

Myriam Labelle, Shahinoor Begum, and Richard O. Hynes

Inventory of Supplemental Information

SUPPLEMENTAL INFORMATION

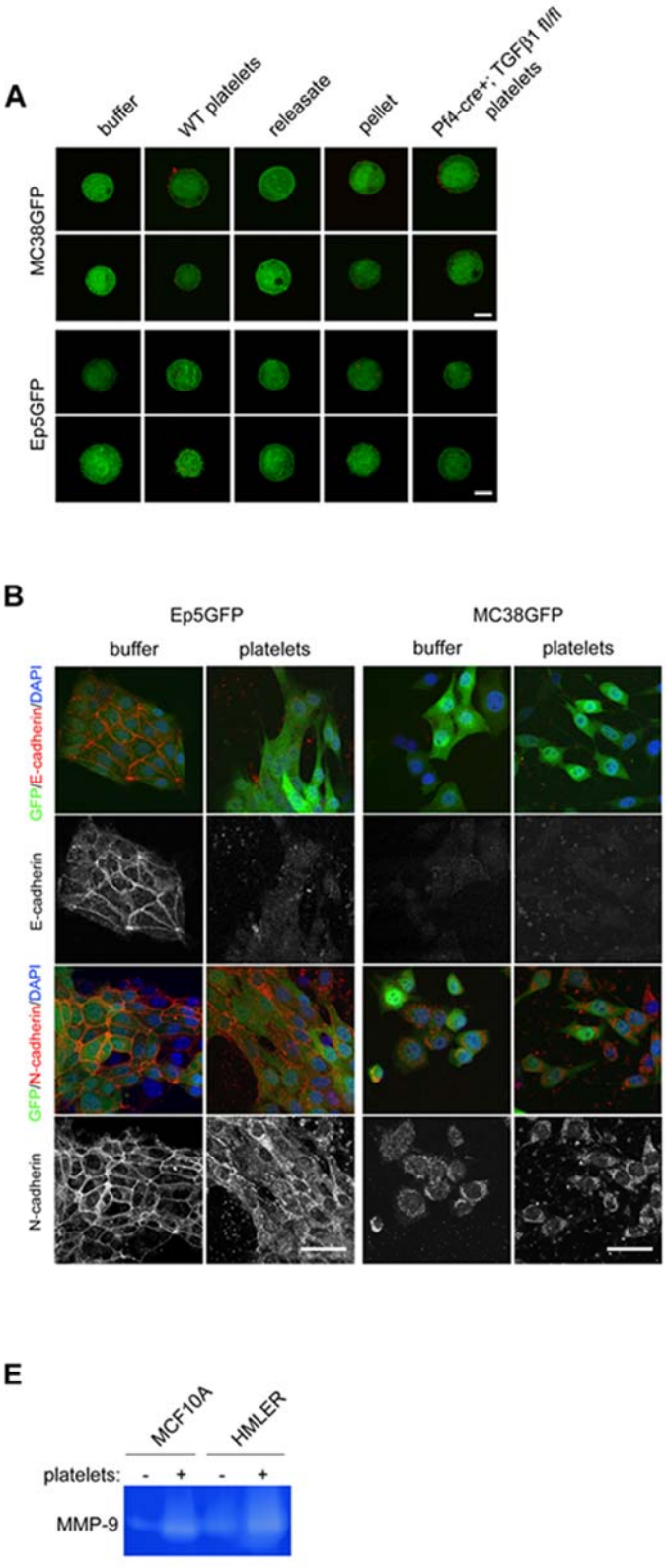

Figure S1, related to Figure 1. Pretreatment of Tumor Cells with Platelets Induces an EMT-Like Phenotype in Mouse and Human Cell Lines.

(A) Immunofluorescence staining for platelets (CD41;red) in cell suspension (prepared as for tail-vein injection) of MC38GFP or Ep5 cells stably expressing GFP. Two representative cells for each condition are shown. Note that very few platelets remain attached to tumor cells treated with platelets or the platelet pellet fraction from WT mice, or with platelets from *Pf4-cre*$^{+}$*;* *TGFβ1*$^{fl/fl}$ mice. Scale bar=10μm.

(B) Immunofluorescence stainings for E-cadherin and N-cadherin (red) in MC38GFP cells or Ep5 cells stably expressing GFP treated with buffer or platelets for 40h. Scale bar=50μm.

(C) Phase-contrast micrographs of MCF10A or HMLER cells treated with buffer or platelets for 24h. Scale bar=50μm.

(D) Relative fold change in mRNA expression in human breast epithelial MCF10A or HMLER human cells treated with buffer or platelets for 40h (n=3). Values are normalized to *GAPDH* expression. Bars represent the mean ± SEM. **p<0.01, ***p<0.001 were determined by Student's t-test.

(E) Zymography for MMP-9 in the conditioned medium of MCF10A or HMLER human cells treated as in (D).

Table S1, related to Figure 2. List of Genes Modulated by More than 2 Fold in Ep5 Cells upon Exposure to Platelets (p<0.05) (Provided as an Excel File)

Table S2, related to Figure 2. List of Genes Modulated by More than 4 fold in Ep5 Cells upon Exposure to Platelets (p<0.05)

Gene Symbol	Log2 fold change	P value
1700112C13Rik	2.098184	1.60E-08
4930572J05Rik	-3.766710667	2.01E-05
9330175M20Rik	-2.024273333	0.000366637
Aldh3a1	-3.059570667	1.60E-05
Ankrd22	-2.472888667	3.88E-06
Arg2	-2.04233	4.25E-05
Atp13a4	-3.085166	1.98E-08
Atp8b1	-2.33801	0.002798052
Bhlhe40	2.119186667	1.36E-08
Bhlhe41	-2.822264667	3.12E-05
C1qtnf1	2.86726	2.56E-10
Ccl2	3.415371333	0.000501074
Chst2	2.286672667	1.05E-08
Cldn1	-2.493964667	3.62E-08
Clu	2.452976667	1.82E-09
Ctsw	5.22753	3.26E-11
Cxcl5	-2.299436667	0.001381252
Edn1	2.325914667	1.57E-05
Eya2	-2.221118667	5.07E-07
Fermt1	2.084543333	9.63E-10
Fn1	2.147283333	4.66E-07
Gm1006	-3.230466	1.20E-07
Gm14203	-2.115369333	1.75E-09
Gpr146	-2.591415333	7.70E-05
Gstt1	-2.132094667	2.31E-06
Id2	-2.530128	0.000104486
Irs1	-2.202704	7.78E-07
Jag1	2.010252	2.09E-06
Klhl1	2.246299333	7.20E-06
Klk6	-3.232498667	3.42E-06
Lrrc26	-3.754262667	6.93E-08
Mcpt8	-2.434465333	2.93E-05
Mgat3	-2.665078667	0.000169619
Mmp3	-2.934538667	3.48E-06
Mmp9	5.549030667	4.86E-11
Mt2	3.137014	3.12E-05
Mxd1	-2.005537333	3.17E-09

Ncam1	3.060405333	2.89E-09
Npnt	-2.537079333	7.44E-06
Nt5e	2.16121	2.99E-05
Padi1	-2.58373	4.09E-07
Pdia5	2.178992	4.35E-05
Ppl	-2.346288	3.27E-05
Rhpn2	-2.334857333	3.05E-07
Rom1	-2.792601333	1.39E-06
Serpinb2	-2.026295333	0.003003047
Serpine1	4.16097	4.47E-09
Sgk2	-3.672803333	1.48E-05
Slc25a35	-2.232655333	0.001304895
Slc26a9	-2.669384667	9.74E-06
Slc44a3	-3.123658	7.31E-05
Styk1	-2.362784	4.20E-06
Tc2n	-2.454634	0.000866249
Tmem71	-2.043573333	0.000126913
Tns4	-2.508330667	7.11E-09
Vegfc	3.681836	1.39E-07
Vim	2.430557333	0.0143674
Wisp1	4.779488	9.59E-11

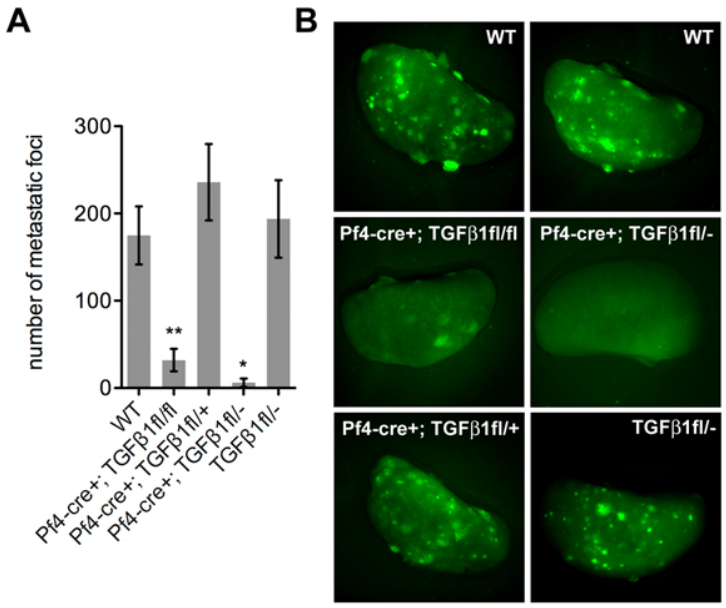

Figure S2, related to Figure 3. *Stumpy* Deletion Does Not Affect Metastasis

(A) Numbers of metastatic foci at the surface of lungs (2 largest lobes) 14 days after tail-vein injection of MC38GFP cells in wild-type (WT), *Pf4-cre*$^{+}$*; TGFβ1*$^{fl/fl}$, *Pf4-cre*$^{+}$*; TGFβ1*$^{fl/+}$ mice, *Pf4-cre*$^{+}$*; TGFβ1*$^{fl/-}$ mice or *TGFβ1*$^{fl/-}$ mice. Each bar represents the mean ± SEM of n=4-9. *p<0.05, **p<0.01 vs WT were determined by one-way ANOVA followed by Tuckey's post test.

(B) Micrographs of lungs 14 days after tail-vein injection of MC38GFP cells in wild-type (WT), *Pf4-cre*$^{+}$*; TGFβ1*$^{fl/fl}$, *Pf4-cre*$^{+}$*; TGFβ1*$^{fl/+}$ mice, *Pf4-cre*$^{+}$*; TGFβ1*$^{fl/-}$ mice, or *TGFβ1*$^{fl/-}$ mice.

Table S3, related to Figure 3. Bleeding Times and Platelet Counts

Genotype	Bleeding time (s)	Platelet count (10^6/μl)
WT	176 ± 27 (n=18)	1.04 ± 0.05 (n=5)
Pf4-cre$^+$*; TGFβ1*$^{fl/fl}$	172 ± 37 (n=6)	1.11 ± 0.16 (n=4)
Pf4-cre$^+$ *; TGFβ1*$^{fl/+}$	187 ± 44 (n=5)	1.12 ± 0.09 (n=5)
Pf4-cre$^+$ *; TGFβ1*$^{fl/-}$	149 ± 19 (n=5)	1.19 ± 0.10 (n=2)
TGFβ1$^{fl/-}$	180 ± 28 (n=7)	0.76 ± 0.16 (n=4)

Bleeding times and platelet counts ± SEM

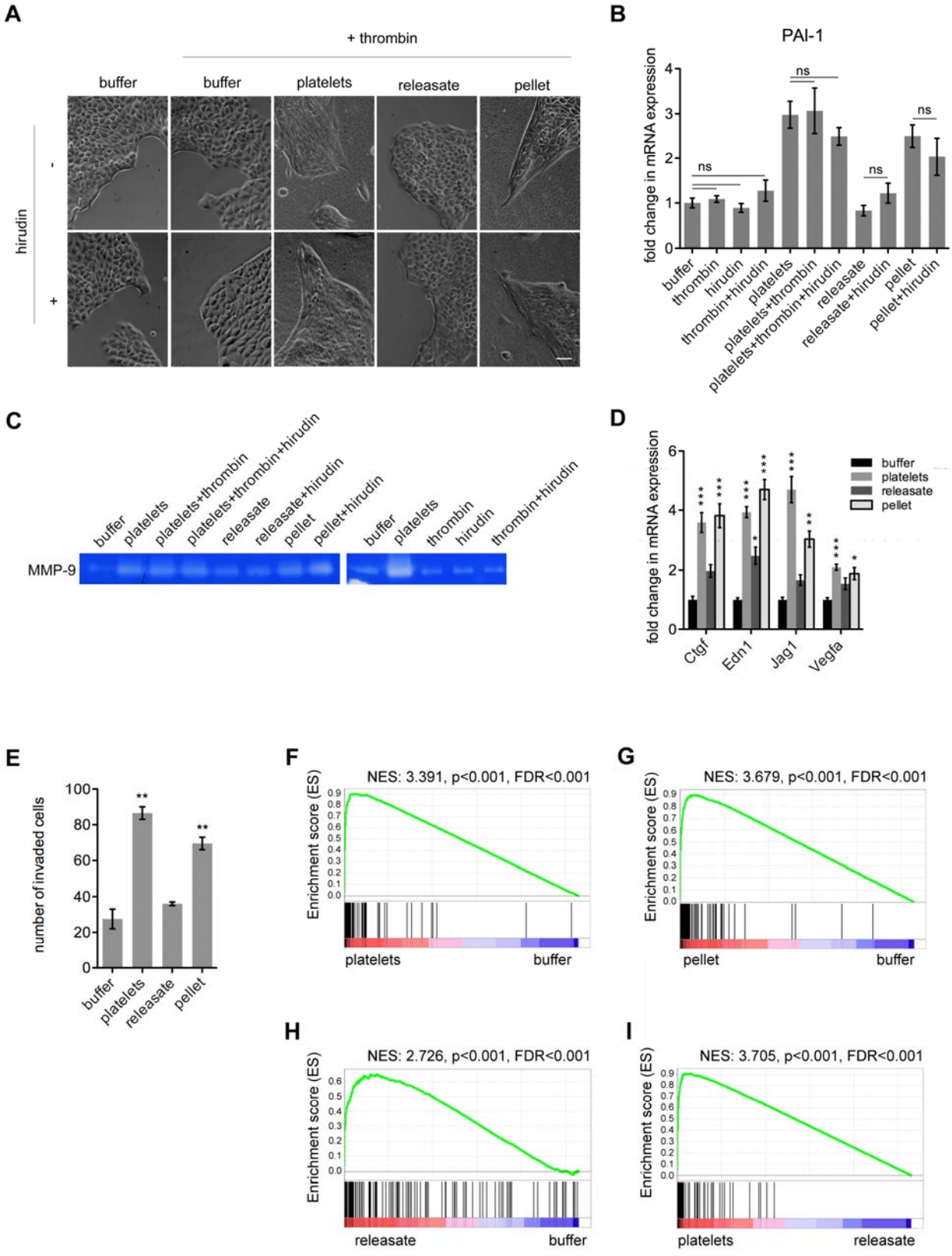
A
+ thrombin
buffer
buffer
platelets
releasate
pellet
hirudin
-
+
B
PAI-1
fold change in mRNA expression
ns
buffer
thrombin
hirudin
thrombin+hirudin
platelets
platelets+thrombin
platelets+thrombin+hirudin
releasate
releasate+hirudin
pellet
pellet+hirudin
C
MMP-9
buffer
platelets
platelets+thrombin
platelets+thrombin+hirudin
releasate
releasate+hirudin
pellet
pellet+hirudin
thrombin
thrombin+hirudin
D
fold change in mRNA expression
buffer
platelets
releasate
pellet
Ctgf
Edn1
Jag1
Vegfa
E
number of invaded cells
F
NES: 3.391, p<0.001, FDR<0.001
Enrichment score (ES)
platelets
buffer
G
NES: 3.679, p<0.001, FDR<0.001
pellet
buffer
H
NES: 2.726, p<0.001, FDR<0.001
releasate
buffer
I
NES: 3.705, p<0.001, FDR<0.001
platelets
releasate

Figure S3, related to Figure 4. Platelet-Derived TGFβ1 and Platelet-Bound Factors Cooperate to Promote Metastasis

(A) Phase-contrast micrographs of Ep5 cells treated with buffer, platelets, releasate from activated platelets (releasate), or the pellet fraction from activated platelets (pellet) +/- thrombin and hirudin for 24h. The releasate and pellet fractions were generated by treating platelets with thrombin (0.5U/ml) and separated by centrifugation. For some conditions, thrombin was blocked with hirudin (5U/ml) prior dilution in culture medium and co-incubation with the tumor cells. Scale bar=50μm.

(B) Relative fold change in *PAI-1* mRNA expression in Ep5 cells treated as in (A) for 40h (n=3). Values are normalized to *Gapdh* expression. ns ($p>0.05$) was determined by one-way ANOVA followed by Tuckey's post test.

(C) Zymography for MMP-9 in the conditioned medium of Ep5 cells treated as in (B).

(D) Relative fold change in mRNA expression in Ep5 cells treated with buffer, platelets, releasate from activated platelets (releasate), or the pellet fraction from activated platelets (pellet) (n=3). Values are normalized to *Gapdh* expression. Bars represent the mean ± SEM, and *$p<0.05$, **$p<0.01$, ***$p<0.001$ vs buffer were determined by one-way ANOVA followed by Tuckey's post test.

(E) Ep5 cells were added at the top of transwells coated with Matrigel and treated with buffer, platelets, releasate from activated platelets (releasate), or the pellet fraction from activated platelets (pellet). The total numbers of cells that invaded to the bottom of the transwell were counted after 48h. Each bar represents the mean ± SEM of n=2. **$p<0.01$ vs buffer were determined by one-way ANOVA followed by Tuckey's post test.

(F-I) Enrichment plots for the platelet-induced gene signature (genes upregulated by more than 2 fold; Table S1) in an independent set of microarray data generated with Ep5 cells treated with

buffer, platelets, releasate from activated platelets (releasate), or the pellet fraction from activated platelets (pellet) (n=3). Enrichment in platelet-, platelet pellet- or releasate-treated cells versus untreated cells (buffer) are shown in F, G and H. Enrichment in the platelet-treated cells in comparison to the releasate-treated cells is presented in I. Each vertical black line represents a platelet-induced gene. The left-to-right position of each line indicates the relative position of the gene within the rank ordering of the 13,243 genes represented in the dataset from the gene most upregulated upon platelet treatment (position 1 on the left) to the most down-regulated (position 13,243 on the right). The genes near the middle are unaffected by the platelet treatment. The platelet-induced gene signature is clearly enriched in the platelet-treated Ep5 cells (E; $p<0.001$, $FDR<0.001$), as evidenced by the cluster of vertical black lines at the very left of the distribution and the positive enrichment score marked by the green line, validating the platelet-induced gene signature in this data set. Similarly, the gene signature is also highly enriched in the pellet-treated cells (F; $p<0.001$, $FDR<0.001$). Interestingly, while the platelet-induced gene signature is overall also enriched in releasate-treated cells (G; $p<0.001$, $FDR<0.001$), there is a subset of genes which are less affected by this treatment and are redistributed towards the right of the plot, suggesting that treatment with the releasate only induces partial gene expression changes in comparison to treatment with platelets in Ep5 cells. The overall lower magnitude of gene expression changes observed in the releasate-treated cells in comparison with platelet-treated cells is further illustrated by the enrichment of the platelet-induced gene signature in platelet-treated cells directly compared to releasate-treated cells (H; $p<0.001$, $FDR<0.001$). The NES (normalized enrichment score), p-value and FDR (false discovery rate) are indicated at the top of each plot.

Table S4, related to Figure 4. Gene Set Enrichment Analysis (GSEA) for Ep5 Cells Treated with Platelets, Platelet Pellet or Platelet Releasate

Gene sets	Platelets vs Buffer			Pellet vs Buffer			Releasate vs Buffer		
	NES	Nominal p-value	FDR	NES	Nominal p-value	FDR	NES	Nominal p-value	FDR
EMT Signatures									
BLICK_EMT-SIG_UP	1.550	0.011	0.044	1.426	0.033	0.063	-1.501	0.018	0.032
TAUBE_EMT_UP	1.430	0.041	0.034	1.220	0.120	0.122	1.024	0.414	0.411
TAUBE_EMT_DN	-1.937	<0.001	0.002	-1.929	<0.001	<0.001	-1.968	<0.001	<0.001
ONDER_CDH1_TARGETS_2_UP	1.470	0.004	0.001	1.350	0.010	0.010	1.093	0.240	0.275
ONDER_CDH1_TARGETS_2_DN	-1.897	<0.001	0.003	-1.863	<0.001	<0.001	-2.058	<0.001	0.002
TGFβ Signatures									
GIAMPIERI_TGFB_UP	2.194	<0.001	<0.001	1.856	<0.001	<0.001	-1.103	0.229	0.221
GIAMPIERI_TGFB_DN	-2.583	<0.001	<0.001	-2.466	<0.001	<0.001	-1.789	<0.001	<0.001
VALCOURT_TGFB_UP	1.976	<0.001	0.002	1.390	0.046	0.039	-1.498	0.013	0.059
VALCOURT_TGFB_DN	-2.130	<0.001	<0.001	-2.162	<0.001	<0.001	-1.725	0.005	0.037
Cancer Stem Cell Signatures									
CREIGHTON_CSC_UP	1.570	0.004	0.001	1.380	0.028	0.021	1.060	0.336	0.313
CREIGHTON_CSC_DN	-1.480	0.004	0.006	-1.540	<0.001	0.002	-1.240	0.063	0.084
Tumor progression and Metastasis Signatures									
VANTVEER_BREAST_CANCER_POOR_PROGNOSIS	1.762	0.004	0.012	1.721	0.005	0.005	1.247	0.155	0.361
JAEGER_METASTASIS_UP	1.790	0.006	0.010	1.663	0.010	0.006	1.273	0.140	0.086
NF-κB Signatures									
HINATA_NFKB_TARGETS_KERATINOCYTE_UP	1.552	0.012	0.046	1.377	0.034	0.074	-1.499	0.026	0.034
SANA_TNF_SIGNALING_UP	1.672	0.007	0.023	1.840	<0.001	<0.001	-1.290	0.083	0.150

Enrichment of gene sets from the literature. Positive normalized enrichment score (NES) indicates enrichment in either platelet-, pellet- or releasate-treated Ep5 cells; negative NES indicates enrichment in untreated Ep5 cells (buffer). FDR (false discovery rate).
NF-κB signatures are enriched in platelet- or pellet-treated Ep5 cells, but not in releasate-treated Ep5 cells (note the negative NES for releasate-treated cells), suggesting a dependence on platelet-bound factors for activation of this pathway. Similarly, while genes upregulated during EMT, upon TGFβ treatment, in cancer stem cells or during tumor progression and metastasis are significantly enriched in platelet- or pellet-treated cells ($p<0.05$ and/or $FDR<0.25$), this enrichment is not observed in releasate-treated cells ($p>0.05$ and/or $FDR>0.25$). However, genes downregulated upon TGFβ treatment and during EMT are significantly depleted upon all three treatments, suggesting that partial TGFβ and EMT responses are maintained in releasate-treated cells.

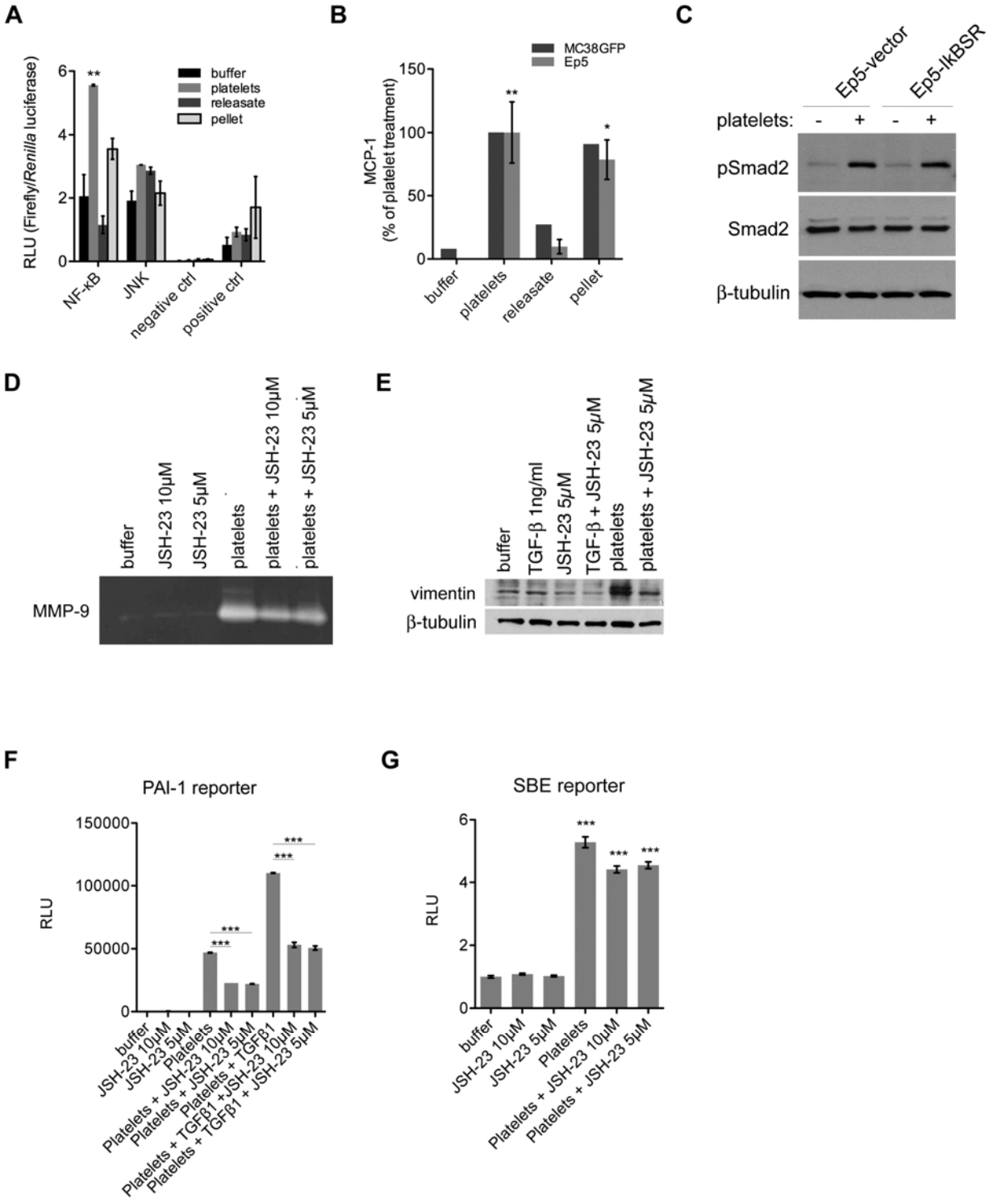
A
RLU (Firefly/Renilla luciferase)
buffer
platelets
releasate
pellet
NF-κB
JNK
negative ctrl
positive ctrl
B
MC38GFP
Ep5
MCP-1
(% of platelet treatment)
buffer
platelets
releasate
pellet
C
Ep5-vector
Ep5-IkBSR
platelets:
pSmad2
Smad2
β-tubulin
D
buffer
JSH-23 10μM
JSH-23 5μM
platelets
platelets + JSH-23 10μM
platelets + JSH-23 5μM
MMP-9
E
buffer
TGF-β 1ng/ml
JSH-23 5μM
TGF-β + JSH-23 5μM
platelets
platelets + JSH-23 5μM
vimentin
β-tubulin
F
PAI-1 reporter
RLU
buffer
JSH-23 10μM
JSH-23 5μM
Platelets
Platelets + JSH-23 10μM
Platelets + JSH-23 5μM
Platelets + TGFβ1
Platelets + TGFβ1 +JSH-23 10μM
Platelets + TGFβ1 + JSH-23 5μM
G
SBE reporter
RLU
buffer
JSH-23 10μM
JSH-23 5μM
Platelets
Platelets + JSH-23 10μM
Platelets + JSH-23 5μM

Figure S4, related to Figure 6. The NF-κB Signaling Pathway Is Activated by Platelets in a Contact-Dependent Manner and Cooperates with TGFβ Signaling to Induce an EMT-Like Transition

(A) Ep5 cells were transfected with firefly luciferase reporters of NF-κB or JNK activity and constitutively active control *Renilla* luciferase reporters. 24h after transfection, the cells were treated with buffer, platelets, releasate from activated platelets (releasate), or the pellet fraction from activated platelets (pellet) for 20h, and the relative luciferase activity (RLU) was measured (n=3).

(B) MCP-1 concentration in the conditioned medium from MC38GFP or Ep5 cells incubated with buffer, platelets, releasate from activated platelets (releasate), or the pellet fraction from activated platelets (pellet) for 40h (n=3).

(C) Detection of phospho-Smad2 and total Smad2 protein levels by immunoblotting in Ep5 cells stably expressing an IκB super-repressor (Ep5-IkBSR) or a control vector (Ep5-vector) and treated with buffer or platelets for 40h. β-tubulin is used as loading control.

(D) Zymography for MMP-9 in the conditioned medium from Ep5 cells treated with buffer, platelets, JSH-23, or platelets + JSH-23 for 40h.

(E) Detection of vimentin protein levels by immunoblotting in Ep5 cells treated with buffer, platelets, JSH-23 5 μM or platelets + JSH-23 5 μM. β-tubulin is used as loading control.

(F) Relative luciferase activity in MLEC cells stably expressing a luciferase reporter under the control of the *PAI-1* promoter construct and treated with buffer, platelets, JSH-23, platelets + JSH-23, or platelets + TGFβ1 (1 ng/ml) + JSH-23 for 20h (n=2).

(G) Relative luciferase activity in Ep5 cells stably expressing a luciferase reporter under the control of the SBE promoter and treated with buffer, platelets, JSH-23 or platelets + JSH-23 for 20h (n=2).

For panels A, B, F and G, bars represent the mean ± SEM, and *p<0.05, **p<0.01, ***p<0.001 vs buffer were determined by one-way ANOVA followed by Tuckey's post test.

SUPPLEMENTAL EXPERIMENTAL PROCEDURES

Tissue Culture

Ep5 (EpRas) cells (obtained from R. Weinberg), MC38GFP cells (obtained from A. Varki), and MLEC cells stably expressing a *PAI-1* promoter-luciferase reporter construct (Abe et al., 1994) were cultivated in DMEM 10% FCS, 1% Penicillin/Streptomycin and 2 mM L-Glutamine. HMLER cells (H-Ras transformed human mammary epithelial cell line; obtained from R. Weinberg) were cultivated as described previously (Elenbaas et al., 2001). MCF10A cells (Soule et al., 1990) were maintained in DMEM/F12 (50:50) supplemented with 5% horse serum, 10mM HEPES, 10µg/ml insulin, 20ng/ml epidermal growth factor, 0.5µg/ml hydrocortisone, 100ng/ml cholera toxin, 1% Penicillin/Streptomycin.

Generation of Cell Lines Stably Expressing ZsGreen and IkBSR Reporters

Retroviral vectors coding for ZsGreen or IκBα super-repressor and GFP (IkBSR) were transduced in Ep5 cells. Packaging of the vectors was obtained by cotransfection of 293FT cells (ATCC) with 1ng transfer vector, 1µg MLV gag-pol, and 1µg VSVg expression vectors using Fugene6 (Roche) as described previously (Stern et al., 2008). 48h after transfection, 293FT cell-conditioned medium was collected, filtered through a 0.45µm filter, and applied to Ep5 cells with 4µg/ml polybrene (Sigma). Ep5 cells were then selected on the basis of GFP or ZsGreen expression by FACS sorting.

Genotyping

DNA from mouse tail biopsies was amplified by PCR using the primers listed in the table below.

Genotyping Primers

For detection of the *Tgfb1* flox and WT alleles	forw rev	5'CCCAGGCTAGCCTTGAACTTCT3' 5'AGGGGTGGAGATGTAGTTTGG3'	(Li et al., 2007)
For simultaneous detection of the *Tgfb1* null (*egfp* knockin) and WT alleles	forw rev1 rev2	5'CGCATCCCACCTTTGCCGAG3' 5'GGCGTCAGCACTAGAAGCCA3' 5'GCCGTAGGTCAG GGTGGTCA3'	(Li et al., 2007)
For detection of the *Pf4-cre* transgene	forw rev	5'CCCATACAGCACACCTTTTG3' 5'TGCACAGTCAGCAGGTT3'	(Tiedt et al., 2007)

***In Vivo* Metastasis Assays**

For lung metastasis assays, cells treated with platelets for 40h were washed in PBS, and either trypsinized (Ep5) or lifted with 2mM EDTA in PBS (MC38GFP). Cells were then rinsed and centrifuged twice to remove platelets, and resuspended in HBSS at a constant number of cells for all mice in a given experiment (250,000 to 1,000,000 cells/injection). 100µl of cell suspension were then injected via the tail vein of syngeneic mice. After 14 days, animals were sacrificed and the numbers of metastatic foci at the surface of lungs were counted under a fluorescence stereomicroscope (Nikon SMZ1500). For 3h and 48h time points, pictures were taken (magnification 3x) and the number of cells/picture was automatically counted with Cell Profiler (Lamprecht et al., 2007). For metastasis experiments with the *Pf4-cre*$^{+}$*; TGFβ1*$^{fl/fl}$ mice, untreated MC38GFP cells cultivated in DMEM 10%FCS were lifted and washed as described above and 100µl of a 1x10E7/ml cell suspension were injected via the tail vein.

RT-qPCR Analysis

RNA was isolated from total cell lysates using RNeasy Mini kit (Qiagen), and reverse-transcribed with TaqMan Reverse Transcription Reagents and random hexameric primers (Applied Biosystems). Human specific PCR primers were designed using Primer3 and BLAST. RT-qPCR was performed with the iQ SYBR Green Supermix (Biorad). Primers used are listed in

the tables below. Data were normalized to *GAPDH* expression. Relative mRNA levels were calculated using the comparative C_T method.

RT-qPCR Primers used with mouse cells

Gapdh forw	5'CAGTATGACTCCACTCACGGC3'
Gapdh rev	5'GAGGGGCCATCCACAGTCTTC3'
Snail forw	5'GGAAGCCCAACTATAGCGAGC3'
Snail rev	5'CAGTTGAAGATCTTCCGCGAC3'
Fibronectin forw	5'CGTAAATTGCCCCATTGAGTG3'
Fibronectin rev	5'GAGGGTCTGCTAACATCACTG3'
Serpine1 (PAI-1) forw	5'CCCGCCTCCTCATCCTGCCT3'
Serpine1 (PAI-1) rev	5'GCCACTGTGCCGCTCTCGTT3'
Claudin-1 forw	5'GCGTTTCGCAAAGCACCGGG3'
Claudin-1 rev	5'GGCTCGGGTTGCCTGCAAAGT3'
Vimentin forw	5'AATGCTTCTCTGGCACGTCT3'
Vimentin rev	5'GCTCCTGGATCTCTTCATCG3'
Slug forw	5'CATCCTTGGGGCGTGTAAGTC3'
Slug Rev	5'GCCCAGAGAACGTAGAATAGGTC3'
Twist forw	5'GGACAAGCTGAGCAAGATTCA3'
Twist rev	5'CGGAGAAGGCGTAGCTGAG3'
Zeb1 forw	5'CGCCATGAGAAGAACGAGGAC3'
Zeb1 rev	5'TGTATGCAAAGGTGTAACTGCAC3'
Zeb2 forw	5'CAGGCTCGGAGACAGATGAAG3'
Zeb2 rev	5'CTTGCAGAATCTCGCCACTG3'
Ctgf forw	5'CTCCACCCGAGTTACCAATG3'
Ctgf rev	5'TGGCGATTTTAGGTGTCC3'
Edn1 forw	5'TTTCCCGTGATCTTCTCTCTGC3'
Edn1 rev	5'CTGAGTTCGGCTCCCAAGAC3'
Jag1 forw	5'TTCAGTTTCGCCTGGCCGAG3'
Jag1 rev	5'TCAGTGTCTGCCATTGCCGG3'
Vegfa forw	5'CTTGTTCAGAGCGGAGAAAGC3'
Vegfa rev	5'ACATCTGCAAGTACGTTCGTT3'

RT-qPCR Primers used with human cells

GAPDH forw	5'GGTCTCCTCTGACTTCAACA3'
GAPDH rev	5'GTGAGGGTCTCTCTCTTCCT3'
Snail forw	5'TCGGAAGCCTAACTACAGCGA3'
Snail rev	5'AGATGAGCATTGGCAGCGAG3'
Fibronectin forw	5'CCATCGCAAACCGCTGCCAT3'
Fibronectin rev	5'AACACTTCTCAGCTATGGGCTT3'
Serpine1 forw	5'ACCGCAACGTGGTTTTCTCA3'

Serpine1 rev	5’TTGAATCCCATAGCTGCTTGAAT3’
N-cadherin forw	5’ATCCTACTGGACGGTTCG3’
N-cadherin rev	5’TTGGCTAATGGCACTTGA3’
Vimentin forw	5’GAACGCCAGATGCGTGAAATG3’
Vimentin rev	5’CCAGAGGGAGTGAATCCAGATTA3’
Slug forw	5’AAGCATTTCAACGCCTCCAAA3’
Slug Rev	5’GGATCTCTGGTTGTGGTATGACA3’
Twist forw	5’CCGGAGACCTAGATGTCATTG3’
Twist rev	5’CCACGCCCTGTTTCTTTG3’
Zeb1 forw	5’GATGATGAATGCGAGTCAGATGC3’
Zeb1 rev	5’ACAGCAGTGTCTTGTTGTTGT3’
Zeb2 forw	5’GGAGACGAGTCCAGCTAGTGT3’
Zeb2 rev	5’CCACTCCACCCTCCCTTATTTC3’

Zymography

Conditioned media from cells treated for 48h were collected and centrifuged to remove cellular debris and platelets. Volumes of conditioned media normalized to the number of cells were then mixed with 2X Laemmli sample buffer (BioRad) and loaded onto a 7.5% acrylamide/bisacrylamide separating gel containing 0.2% (w/v) gelatin. After electrophoresis, the gel was incubated in 2.5% Triton X-100, rinsed in distilled water and incubated at 37°C in buffer containing 50mM Tris pH 7.6, 20mM NaCl, 5mM $CaCl_2$. Finally, the gel was stained in 0.1% Coomassie blue R-250, 30% methanol, 10% acetic acid, and destained in the same solution without the Coomassie blue dye.

Immunoblotting

Immunoblot analysis was performed as described previously (Labelle et al., 2008). The primary antibodies were anti-β-tubulin (Sigma), anti E-cadherin (BD Biosciences), anti-Smad2/3, anti-phosphoSmad2 (Cell Signaling Technology) and anti-vimentin (Sigma). The secondary antibodies were horseradish peroxidase-conjugated anti-rabbit or anti-mouse IgG (Jackson

Immunoresearch).

Invasion Assay

Invasion assays were performed in 24-well BD Biocoat™ Matrigel™ Invasion Chambers (8 μm pore size; BD Biosciences). 50,000 cells were plated in transwell inserts and either left untreated, treated with SB431542 (10 μM), anti-TGFβ1 blocking antibody (6μg/ml) or the different platelet fractions. Both upper and lower chambers contained DMEM. After 48h, cells remaining in the upper part of the transwell were removed with a cotton swab. Migrated cells were then stained with Crystal Violet 0.5% and the total number of cells was counted with a Zeiss Axiovert 200 microscope.

Immunofluorescence Staining

For visualization of blood vessels and quantification of extravasation, lungs were fixed by tracheal perfusion with PBS, 4% formaldehyde, 0.3% Triton X-100 for 15 min and removed en bloc. Lung lobes were then cut in 4 pieces, washed in PBS, 0.3% triton X-100 and blocked in PBS 10% normal goat serum followed by the primary antibody (anti-PECAM-1, BD Biosciences). After washing, samples were incubated with Alexa 594-conjugated goat anti-rat IgG (Molecular probes) and DAPI. Images of lobe pieces from 3 or more mice per group were taken at 60X with Z-sections every 1μm on an Olympus FV10i inverted confocal microscope. 3D rendering and XYZ views were generated with Volocity (Perkin Elmer). XYZ views were then examined and cells clearly within blood vessels (directly surrounded by PECAM-1 staining; red) were scored as intravascular, while cells outside blood vessels were scored as extravascular.

For platelet immunostaining in lungs, 20 μm-thick sections were fixed in acetone and stained

with anti-GP1bβ (Emfret). The secondary antibody was Alexa 594-conjugated goat anti-rat IgG (Molecular Probes). Images were taken at 60X with Z-sections every 1μm on an Olympus FV10i inverted confocal microscope.

For platelet immunostaining in cell suspensions, cells were prepared as for *in vivo* metastasis assays. The suspensions were then stained with anti-CD41 (BD Biosciences), washed once with PBS and incubated with Alexa 594-conjugated goat anti-rat IgG (Molecular probes). After a final wash in PBS, cells were resuspended in PBS and 5μl of cell suspensions were loaded on a microscope slide.

For immunostaining of tumor cells in tissue culture, cells were rinsed with PBS, fixed with 4% formaldehyde and stained with anti-E-cadherin or anti-N-cadherin (BD Biosciences). The secondary antibody was Alexa 594-conjugated goat anti-rat IgG (Molecular probes). Images were taken with a Zeiss LSM510 microscope.

Tail Bleeding Assay

For tail bleeding assays, mice were anesthetized with 2.5% isoflurane in oxygen. The tail was cut at 5mm and bled onto a Whatman filter paper. The filter paper was dabbed to the wound every 30 seconds without disrupting the forming clot. The experiment was continued until bleeding stopped completely.

Microarray Analysis

For data presented in Fig. S3 and Table S4, total RNA was isolated from Ep5 cells treated with buffer, platelets, platelet pellet or platelet releastate (n=3). Samples where then processed with

the Nugen Applause® WT-Amp Plus ST System and hybridized on Affymetrix Mouse Gene 1.0 ST arrays, according to manufacturer's instructions (Affymetrix).

Data are deposited in Gene Expression Omnibus (GEO) under accession number GSE27456.

Gene Set Enrichment Analysis (GSEA)

GSEA was performed using GSEA v2.07 (www.broadinstitute.org/gsea; Mootha et al., 2003; Subramanian et al., 2005). The signal-to-noise metric and permutation of gene sets were used to rank the genes and calculate nominal p-values and FDR. Probe sets were collapsed to unique gene symbols and used to interrogate the gene sets from the literature listed in the table below, some of which were provided by the Molecular Signatures Database (MSigDB; www.broadinstitute.org/gsea/msigdb).

Gene set	Source
BLICK_EMT-SIG	(Blick et al.)
TAUBE_EMT	(Taube et al.)
ONDER_CDH1_TARGETS_2	MSigDB, (Onder et al., 2008)
GIAMPIERI_TGFB	(Giampieri et al., 2009)
VALCOURT_TGFB	(Valcourt et al., 2005)
HINATA_NFKB_TARGETS_KERATINOCYTE	MSigDB, (Hinata et al., 2003)
SANA_TNF_SIGNALING	MSigDB, (Sana et al., 2005)
CREIGHTON_CSC	(Creighton et al., 2009)
VANTVEER_BREAST_CANCER_POOR_PROGNOSIS	MSigDB, (van 't Veer et al., 2002)
JAEGER_METASTASIS	MSigDB, (Jaeger et al., 2007)

SUPPLEMENTAL REFERENCES

Blick, T., Hugo, H., Widodo, E., Waltham, M., Pinto, C., Mani, S.A., Weinberg, R.A., Neve, R.M., Lenburg, M.E., and Thompson, E.W. Epithelial mesenchymal transition traits in human breast cancer cell lines parallel the CD44(hi/)CD24 (lo/-) stem cell phenotype in human breast cancer. J Mammary Gland Biol Neoplasia *15*, 235-252.

Creighton, C.J., Li, X., Landis, M., Dixon, J.M., Neumeister, V.M., Sjolund, A., Rimm, D.L., Wong, H., Rodriguez, A., Herschkowitz, J.I.*, et al.* (2009). Residual breast cancers after conventional therapy display mesenchymal as well as tumor-initiating features. Proc Natl Acad Sci U S A *106*, 13820-13825.

Elenbaas, B., Spirio, L., Koerner, F., Fleming, M.D., Zimonjic, D.B., Donaher, J.L., Popescu, N.C., Hahn, W.C., and Weinberg, R.A. (2001). Human breast cancer cells generated by oncogenic transformation of primary mammary epithelial cells. Genes Dev *15*, 50-65.

Hinata, K., Gervin, A.M., Jennifer Zhang, Y., and Khavari, P.A. (2003). Divergent gene regulation and growth effects by NF-kappa B in epithelial and mesenchymal cells of human skin. Oncogene *22*, 1955-1964.

Jaeger, J., Koczan, D., Thiesen, H.J., Ibrahim, S.M., Gross, G., Spang, R., and Kunz, M. (2007). Gene expression signatures for tumor progression, tumor subtype, and tumor thickness in laser-microdissected melanoma tissues. Clin Cancer Res *13*, 806-815.

Lamprecht, M.R., Sabatini, D.M., and Carpenter, A.E. (2007). CellProfiler: free, versatile software for automated biological image analysis. Biotechniques *42*, 71-75.

Mootha, V.K., Lindgren, C.M., Eriksson, K.F., Subramanian, A., Sihag, S., Lehar, J., Puigserver, P., Carlsson, E., Ridderstrale, M., Laurila, E.*, et al.* (2003). PGC-1alpha-responsive genes involved in oxidative phosphorylation are coordinately downregulated in human diabetes. Nat Genet *34*, 267-273.

Onder, T.T., Gupta, P.B., Mani, S.A., Yang, J., Lander, E.S., and Weinberg, R.A. (2008). Loss of E-cadherin promotes metastasis via multiple downstream transcriptional pathways. Cancer Res *68*, 3645-3654.

Sana, T.R., Janatpour, M.J., Sathe, M., McEvoy, L.M., and McClanahan, T.K. (2005). Microarray analysis of primary endothelial cells challenged with different inflammatory and immune cytokines. Cytokine *29*, 256-269.

Soule, H.D., Maloney, T.M., Wolman, S.R., Peterson, W.D., Jr., Brenz, R., McGrath, C.M., Russo, J., Pauley, R.J., Jones, R.F., and Brooks, S.C. (1990). Isolation and characterization of a spontaneously immortalized human breast epithelial cell line, MCF-10. Cancer Res *50*, 6075-6086.

Subramanian, A., Tamayo, P., Mootha, V.K., Mukherjee, S., Ebert, B.L., Gillette, M.A., Paulovich, A., Pomeroy, S.L., Golub, T.R., Lander, E.S.*, et al.* (2005). Gene set enrichment

analysis: a knowledge-based approach for interpreting genome-wide expression profiles. Proc Natl Acad Sci U S A *102*, 15545-15550.

Taube, J.H., Herschkowitz, J.I., Komurov, K., Zhou, A.Y., Gupta, S., Yang, J., Hartwell, K., Onder, T.T., Gupta, P.B., Evans, K.W.*, et al.* Core epithelial-to-mesenchymal transition interactome gene-expression signature is associated with claudin-low and metaplastic breast cancer subtypes. Proc Natl Acad Sci U S A *107*, 15449-15454.

Valcourt, U., Kowanetz, M., Niimi, H., Heldin, C.H., and Moustakas, A. (2005). TGF-beta and the Smad signaling pathway support transcriptomic reprogramming during epithelial-mesenchymal cell transition. Mol Biol Cell *16*, 1987-2002.

van 't Veer, L.J., Dai, H., van de Vijver, M.J., He, Y.D., Hart, A.A., Mao, M., Peterse, H.L., van der Kooy, K., Marton, M.J., Witteveen, A.T.*, et al.* (2002). Gene expression profiling predicts clinical outcome of breast cancer. Nature *415*, 530-536.